Supplementary Material

Room Temperature Proton Coupled Energy Transfer

Chih-Hsing Wang[1,†], Ying-Yi Tsai[1,†], Sheng-Fu Wang[1,†], Chao-Hsien Hsu[1,†], Chien-Yu Lai[1,†], Yu-Chen Wei[1], Chih-Pin Han[1], Hao-Ting Qu[1], Yi-Ching Chan[1], Yu-Sheng Tsai Yuan[1], Yuan-Chung Cheng[1], Liang-Yan Hsu[1,3,4,*], Chao-Tsen Chen[1,2,*], Pi-Tai Chou[1,2,*]

[1]Department of Chemistry, National Taiwan University; Taipei, 10617, Taiwan.

[2]Center for Emerging Material and Advanced Devices, National Taiwan University, Taipei 10617, Taiwan.

[3]Institute of Atomic and Molecular Sciences, Academia Sinica, Taipei 106, Taiwan

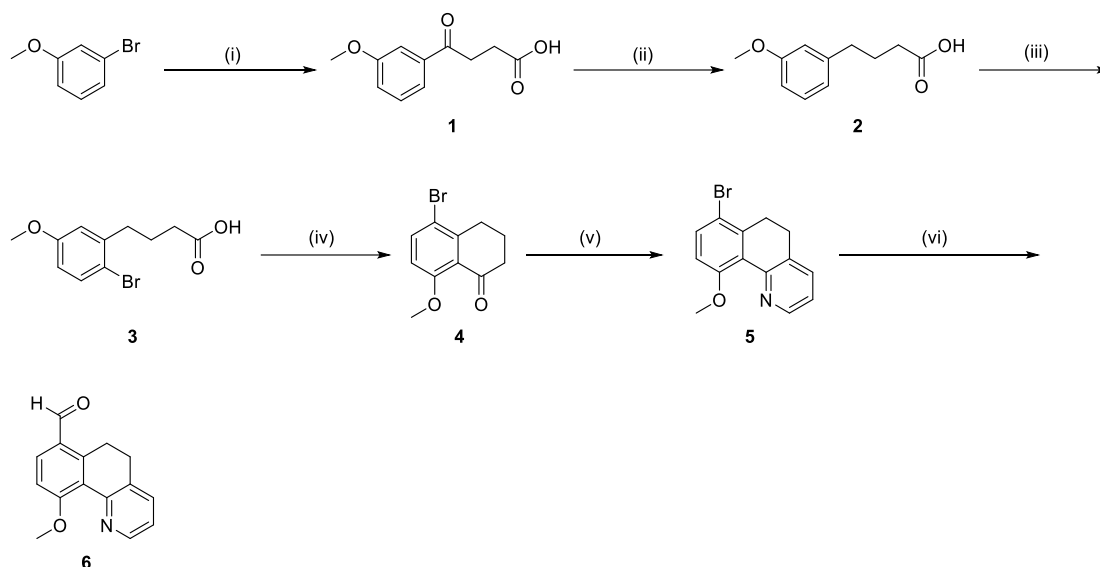[4]Physics Division, National Center for Theoretical Sciences, Taipei 106, Taiwan

*Corresponding author. Email: chop@ntu.edu.tw (P.-T.C.); lyhsu@gate.sinica.edu.tw (L.-Y.H.); chenct@ntu.edu.tw (C.-T.C.)

†These authors contributed equally to this work.

Table of contents

1. Synthesis

Scheme S1. (i) Mg, THF, reflux, 3 h, then succinic anhydride, -40 to RT, 12 h (ii) KOH, N_2H_4, ethylene glycol, 80°C to reflux, 12 h (iii) Br_2, AcOH, 0 to RT, 12 h (iv) H_2SO_4, 80°C, 2 h (v) propargyl amine, $CuCl_2$, IPA, 50°C to reflux, 24h (vi) n-BuLi, DMF, THF, -78°C to RT, 3 h

4-(3-methoxyphenyl)-4-oxobutanoic acid (1). Magnesium turnings (1.6 g, 64.2 mmol) were introduced into anhydrous THF (30 mL) along with a small crystal of iodine. After stirring for 10 minutes, a solution of 3-bromoanisole (10.0 g, 54.5 mmol) in anhydrous THF (20 mL) was added dropwise via an addition funnel. The reaction mixture was subsequently heated under reflux for 3 hours to form the relevant Grignard reagent. Meanwhile, in a separate flask, succinic anhydride (4.9 g, 48.6 mmol) was dissolved in anhydrous THF (50 mL) and cooled to −40 °C. The freshly prepared Grignard reagent was then introduced dropwise via an addition funnel at the same temperature. Upon completion, the reaction mixture was gradually warmed to room temperature and stirred for an additional 12 hours to ensure complete conversion. The reaction was then acidified to pH = 1 using 12N aqueous HCl, after which the solvent was concentrated to remove most of the THF. The resulting residue was extracted multiple times with ethyl acetate and water until no product remained in the aqueous phase. The combined organic layers were subsequently dried over anhydrous $MgSO_4$, followed by concentration under reduced pressure. Finally, the crude product was purified via column chromatography (ethyl acetate/hexane = 1:3), yielding a white solid (7.7 g, 69%). ^{1}H NMR (400 MHz, CDCl$_3$) δ 7.60-7.53 (m, 1H), 7.52-7.48 (m, 1H), 7.38 (t, J = 7.9 Hz, 1H), 7.16-7.09 (m, 1H), 3.86 (s, 3H), 3.30 (t, J = 8.0 Hz, 2H), 2.81 (t, J = 8.0 Hz, 2H). The observed NMR shifts are in agreement with literature values. [1]

4-(3-methoxyphenyl)butanoic acid (2). To a solution of compound **1** (7.7 g, 37 mmol) in ethylene

glycol (40 mL), finely powdered KOH (16.6 g, 296 mmol) was added. The mixture was then heated to 80°C until complete dissolution of all materials. Subsequently, hydrazine monohydrate (15 mL) was introduced into the reaction mixture via syringe, and the reaction was heated under reflux for 12 hours to ensure full conversion. Upon completion, the reaction mixture was poured onto crushed ice and acidified to pH = 1 using 12N aqueous HCl. The resulting mixture was then extracted several times with ethyl acetate and water. The combined organic layers were dried over anhydrous $MgSO_4$ and concentrated under reduced pressure. Finally, the crude product was purified via column chromatography (ethyl acetate/hexane = 1:4), affording a white solid (5.1 g, 71%). ^{1}H NMR (400 MHz, CDCl$_3$) δ 10.05 (s, 1H), 7.24-7.18 (m, 1H), 6.82-6.73 (m, 3H), 3.81 (s, 3H), 2.66 (t, J = 7.4 Hz, 2H), 2.39 (t, J = 7.4 Hz, 2H), 1.98 (quin, J = 7.5 Hz, 2H). The observed NMR shifts are in agreement with literature values. [1]

4-(2-bromo-5-methoxyphenyl)butanoic acid (3). A solution of compound **2** (5.1 g, 26.3 mmol) in acetic acid (40 mL) was cooled to 0°C. Subsequently, a solution of bromine (1.5 mL, 28.9 mmol) in acetic acid (10 mL) was added dropwise via an addition funnel. Upon complete addition, the reaction mixture was gradually warmed to room temperature and stirred for 12 hours. After completion, the reaction mixture was poured onto crushed ice and a substantial amount white solid precipitated out. The solid was collected by filtration, washed several times with cold water to remove residual impurities, and then dried under vacuum, affording a white solid (7.0 g, 98%). ^{1}H NMR (400 MHz, CDCl$_3$) δ 7.41 (d, J = 8.7 Hz, 1H), 6.77 (s, 1H), 6.64 (d, J = 8.8 Hz, 1H), 3.78 (s, 3H), 2.76 (t, J = 7.9 Hz, 2H), 2.43 (t, J = 7.6 Hz, 2H), 1.97 (quin, J = 7.6 Hz, 2H). ^{13}C NMR (100.6 MHz, CDCl$_3$) δ 179.6, 159.1, 141.7, 133.6, 116.3, 115.1, 113.6, 55.6, 35.6, 33.5, 24.9.

5-bromo-8-methoxy-3,4-dihydronaphthalen-1(2H)-one (4). Compound **3** (7.0 g, 25.6 mmol) was slowly added to sulfuric acid (30 mL) under continuous stirring. The reaction mixture was then heated to 80°C and maintained at this temperature for 2 hours to ensure complete reaction. Subsequently, the mixture was allowed to cool to room temperature and was then poured onto crushed ice. The resulting solution was extracted several times with ethyl acetate, followed by additional extractions of the organic phase with water to remove any remaining sulfuric acid. The combined organic layers were dried over anhydrous $MgSO_4$ and concentrated under reduced pressure. Finally, the crude product was purified by column chromatography (ethyl acetate/hexane = 1:5), affording a brown syrup (5.8 g, 89%). ^{1}H NMR (400 MHz, CDCl$_3$) δ 7.63 (d, J = 9.0 Hz, 1H), 6.76 (d, J = 9.0 Hz, 1H), 3.88 (s, 3H), 2.96 (t, J = 6.3 Hz, 2H), 2.64-2.59 (m, 2H), 2.12-2.05 (m, 2H). The observed NMR shifts are in agreement with literature values. [2]

7-bromo-10-methoxy-5,6-dihydrobenzo[h]quinoline (5). A solution of propargyl amine (2.5 g, 45.5 mmol) in isopropanol (75 mL) was preheated to 50°C. Subsequently, compound **4** (5.8 g, 22.7 mmol) and anhydrous $CuCl_2$ (153 mg, 1.14 mmol) were successively added to the amine solution under

continuous stirring. The reaction mixture was then heated to reflux under air for 24 hours to ensure complete conversion. Upon completion, the insoluble salt was removed by filtration, and the filtrate was concentrated under reduced pressure. The resulting residue was then extracted sequentially with ethyl acetate and water. The combined organic layers were dried over anhydrous $MgSO_4$ and concentrated in vacuo. Finally, the crude product was purified by column chromatography (ethyl acetate/hexane = 1:1), affording a tan solid (5.1 g, 59%). ^{1}H NMR (400 MHz, $CDCl_3$) δ 8.62 (dd, $J =$ 4.8, 1.8 Hz, 1H), 7.60-7.52 (m, 1H), 7.50 (d, $J =$ 8.9 Hz, 1H), 7.13 (dd, $J =$ 7.6, 2.4 Hz, 1H), 6.87 (d, $J =$ 8.9 Hz, 1H), 3.92 (s, 3H), 2.99-2.93 (m, 2H), 2.83-2.77 (m, 2H). ^{13}C NMR (100.6 MHz, $CDCl_3$) δ 157.6, 152.2, 147.4, 140.9, 135.2, 133.8, 133.6, 125.8, 122.2, 114.6, 113.0, 56.9, 29.3, 28.6. MS (HRFD) calcd. for $C_{14}H_{12}NOBr$ [M[+]]: m/z: 289.0097, Found: 289.0100.

10-methoxy-5,6-dihydrobenzo[*h*]quinoline-7-carbaldehyde (6). Compound **5** (1.0 g, 3.4 mmol) in dry THF (15 mL) was cooled to -78°C using a dry ice/acetone bath. To this solution, 1.6 M n-BuLi (2.4 mL, 3.8 mmol) was added dropwise via syringe, and the reaction mixture was stirred at the same temperature for 1 hour. Subsequently, dry DMF (0.49 mL, 5.9 mmol) was added dropwise via syringe, and the reaction mixture was allowed to warm to room temperature. Stirring was continued at room temperature for an additional 2 hours. The reaction was then quenched by the addition of saturated $NH_4Cl_{(aq.)}$, and the solvent was removed under reduced pressure. The residue was extracted with ethyl acetate and water, and the combined organic layers were dried over anhydrous $MgSO_4$ before being concentrated in vacuo. Finally, the crude product was purified by column chromatography (ethyl acetate/hexane = 1:1), affording a beige solid (640 mg, 78%). ^{1}H NMR (400 MHz, $CDCl_3$) δ 10.17 (s, 1H), 8.61 (dd, $J =$ 4.8, 1.8 Hz, 1H), 7.84 (d, $J =$ 8.7 Hz, 1H), 7.55 (dd, $J =$ 7.6, 1.8 Hz, 1H), 7.16 (dd, $J =$ 7.5, 4.8 Hz, 1H), 7.09 (d, $J =$ 8.7 Hz, 1H), 4.01 (s, 3H), 3.37-3.31 (m, 2H), 2.83-2.77 (m, 2H). ^{13}C NMR (100.6 MHz, $CDCl_3$) δ 191.5, 162.4, 151.6, 147.4, 145.2, 135.7, 134.9, 134.0, 126.6, 124.7, 122.3, 110.7, 56.7, 28.3, 24.0. MS (HRFD) calcd. for $C_{15}H_{13}NO_2$ [M[+]]: m/z: 239.0941, Found: 239.0938.
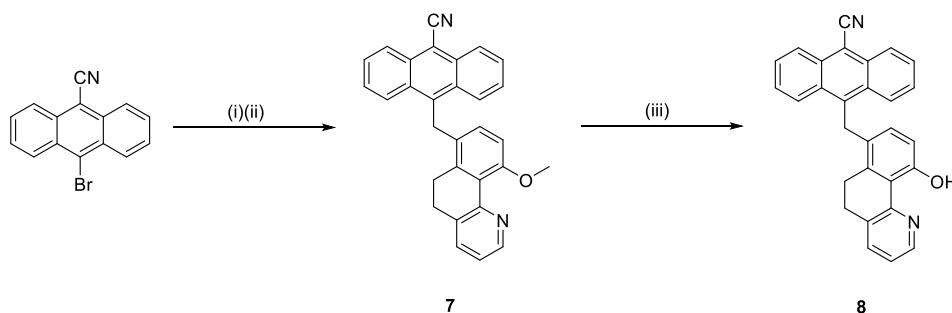
Scheme S2. (i) n-BuLi, **6**, THF, -78°C to RT (ii) Et_3SiH, $BF_3 \cdot Et_2O$, CH_2Cl_2, -78°C to RT, 12 h. (iii) BBr_3, CH_2Cl_2, -78°C to RT, 6 h.
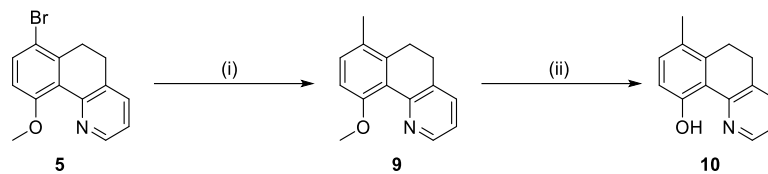
10-((10-methoxy-5,6-dihydrobenzo[*h*]quinolin-7-yl)methyl)anthracene-9-carbonitrile (7) 10-

Bromoanthracene-9-carbonitrile (1.0 g, 3.5 mmol) was dissolved in dry THF (15 mL) and cooled to -78°C using a dry ice/acetone bath. To this solution, 1.6 M n-BuLi (2.7 mL, 4.3 mmol) was added dropwise via syringe, and the reaction mixture was stirred at the same temperature for 1 hour. Subsequently, compound **6** (706 mg, 3.0 mmol) in dry THF (10 mL) was added dropwise to the reaction mixture via an additional funnel. The reaction mixture was then allowed to warm to room temperature and stirred for 12 hours. The reaction was quenched by the addition of saturated $NH_4Cl_{(aq.)}$, and the solvent was concentrated under reduced pressure. The residue was extracted with ethyl acetate and water, and the combined organic layer was dried over anhydrous $MgSO_4$ before being concentrated in vacuo. The crude product was further purified by column chromatography (ethyl acetate/hexane = 1:1), affording the hydroxyl intermediate as a yellow solid. The hydroxyl intermediate was then dissolved in dry CH_2Cl_2 (50 mL) and cooled to -78°C using a dry ice/acetone bath. To this solution, triethylsilane (2.4 mL, 14.8 mmol) was added dropwise, and the mixture was stirred at the same temperature for 5 minutes. Subsequently, boron trifluoride etherate (1.8 mL, 14.8 mmol) was added dropwise to the reaction mixture, which was then allowed to warm to room temperature and stirred for 12 hours. The reaction was quenched by adding water, and the mixture was extracted with CH_2Cl_2 and water. The combined organic layers were dried over anhydrous $MgSO_4$ and concentrated in vacuo. The crude product was further purified by column chromatography (MeOH/ethyl acetate/hexane = 5:50:50), affording a pale yellow solid (980 mg, 77%). ^1H NMR (400 MHz, DMSO-d_6) δ 8.52 (dd, J = 4.9, 1.8 Hz, 1H), 8.39 (d, J = 8.6 Hz, 2H), 8.33 (d, J = 8.9 Hz, 2H), 7.90-7.84 (m, 2H), 7.80 (d, J = 7.6 Hz, 1H), 7.71-7.64 (m, 2H), 7.29 (dd, J = 7.6, 4.9 Hz, 1H), 6.63 (d, J = 8.7 Hz, 1H), 5.94 (d, J = 8.6 Hz, 1H), 5.06 (s, 2H), 3.63 (s, 3H), 3.20-3.15 (m, 2H), 3.00-2.94 (m, 2H). ^{13}C NMR (100.6 MHz, DMSO-d_6) δ 156.2, 140.9, 140.1, 133.6, 132.5, 129.7, 129.5, 129.0, 127.2, 126.3, 125.3, 122.0, 122.0, 117.2, 111.2, 104.0, 55.9, 30.9, 28.0, 24.6. MS (HRFD) calcd. for $C_{30}H_{22}N_2O$ [M^+]: m/z: 426.1727, Found: 426.1731. Crystals suitable for X-ray diffraction were obtained from a mixture of CH_2Cl_2 and hexane at room temperature.

10-((10-hydroxy-5,6-dihydrobenzo[*h*]quinolin-7-yl)methyl)anthracene-9-carbonitrile (8)
Compound **7** (500 mg, 1.2 mmol) was dissolved in dry CH_2Cl_2 (20 mL) and cooled to -78°C using a dry ice/acetone bath. To this solution, BBr$_3$ (0.33 mL, 3.5 mmol) diluted in dry CH_2Cl_2 (3.5 mL) was added slowly. The reaction mixture was then allowed to warm to room temperature and stirred for 6 hours. The reaction was quenched by the addition of water, and the mixture was extracted with CH_2Cl_2 and water. The combined organic layers were dried over anhydrous $MgSO_4$ and concentrated under reduced pressure. The crude product was further purified by column chromatography (ethyl acetate/hexane = 1:1), affording a yellow solid (236 mg, 49%). ^1H NMR (400 MHz, CDCl$_3$) δ 14.16 (br, 1H), 8.51 (d, J = 8.6 Hz, 2H), 8.39 (dd, J = 5.0, 1.7 Hz, 1H), 8.15 (d, J = 8.9 Hz, 2H), 7.75-7.64 (m, 3H), 7.58-7.50 (m, 2H), 7.22 (dd, J = 7.6, 5.0 Hz, 1H), 6.51 (d, J = 8.6 Hz, 1H), 6.16 (d, J = 8.6 Hz, 1H), 4.92 (s, 2H), 3.36-3.28 (m, 2H), 3.22-3.14 (m, 2H). ^{13}C NMR (100.6 MHz, DMSO-d_6) δ 157.1, 153.6, 144.1, 141.0, 137.0, 136.9, 132.4, 131.8, 130.0, 129.6, 129.4, 127.1, 126.9, 126.1, 125.2,

122.3, 117.1, 116.0, 114.9, 104.0, 30.2, 26.5, 23.4. MS (HRFD) calcd. for $C_{29}H_{20}N_2O$ [M$^+$]: m/z: 412.1570, Found: 412.1575. Crystals suitable for X-ray diffraction were obtained from a mixture of CH_2Cl_2 and hexane at room temperature.

Scheme S3. (i) MeB(OH)$_2$, K$_2$CO$_3$, Pd(dppf)Cl$_2$, THF, H$_2$O, reflux, 12 h. (ii) BBr$_3$, CH$_2$Cl$_2$, -78°C to RT, 6 h.

10-methoxy-7-methyl-5,6-dihydrobenzo[*h*]quinoline (9). A flask containing compound **5** (640 mg, 2.2 mmol), K$_2$CO$_3$ (910 mg, 6.7 mmol), methylboronic acid (400 mg, 6.7 mmol), and Pd(dppf)Cl$_2$ (81 mg, 0.1 mmol) was degassed and backfilled with nitrogen, repeat this process three times. Subsequently, degassed THF (9 mL) and water (3 mL) were added to dissolve the reaction mixture, which was then heated to reflux for 12 hours. Upon completion of the reaction, the mixture was extracted with ethyl acetate and water. The combined organic layers were dried over anhydrous MgSO$_4$ and concentrated under reduced pressure. The crude product was further purified by column chromatography (ethyl acetate/hexane = 1:1), yielding a viscous amber oil (490 mg, 99%), which solidified after refrigeration. ^{1}H NMR (400 MHz, CDCl$_3$) δ 8.60 (dd, J = 4.9, 1.8 Hz, 1H), 7.52 (dd, J = 7.5, 1.8 Hz, 1H), 7.15 (d, J = 4.5 Hz, 1H), 7.10 (dd, J = 7.5, 4.9 Hz, 1H), 6.87 (d, J = 8.4 Hz, 1H), 3.90 (s, 3H), 2.82-2.71 (m, 4H), 2.28 (s, 3H). ^{13}C NMR (100.6 MHz, CDCl$_3$) δ 156.5, 153.0, 147.1, 140.3, 135.0, 133.8, 131.7, 126.9, 123.5, 121.6, 110.9, 56.6, 28.7, 25.5, 19.6. MS (HRFD) calcd. for $C_{15}H_{15}NO$ [M$^+$]: m/z: 225.1148, Found: 225.1152.

7-methyl-5,6-dihydrobenzo[*h*]quinolin-10-ol (10). Compound **10** was synthesized using a procedure similar to that employed for the synthesis of compound **8**. (Yield: 82%). ^{1}H NMR (400 MHz, CDCl$_3$) δ 14.18 (br, 1H), 8.42 (dd, J = 5.1, 1.6 Hz, 1H), 7.65 (d, J = 7.5 Hz, 1H), 7.21 (dd. J = 7.6, 5.1 Hz, 1H), 7.10 (d, J = 8.4 Hz, 1H), 6.92 (d, J = 8.4 Hz, 1H), 3.91-2.94 (m, 2H), 2.93-2.85 (m, 2H), 2.25 (s, 3H). ^{13}C NMR (100.6 MHz, CDCl$_3$) δ 157.8, 154.9, 144.0, 136.8, 136.2, 133.1, 124.9, 121.5, 116.5, 115.5, 27.7, 24.3, 19.3. MS (HRFD) calcd. for $C_{14}H_{13}NO$ [M$^+$]: m/z: 211.0992, Found: 211.0995.
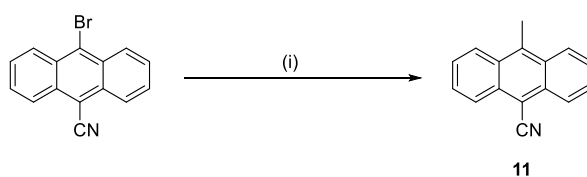
Scheme S4. (i) MeB(OH)$_2$, K$_2$CO$_3$, Pd(dppf)Cl$_2$, dioxane, H$_2$O, reflux, 12 h.

10-methylanthracene-9-carbonitrile (11). A flask containing compound **11** (1.2g, 4.25 mmol), K_2CO_3 (1.8 g, 12.8 mmol), methylboronic acid (763 mg, 12.8 mmol), and $Pd(dppf)Cl_2$ (93 mg, 0.89 mmol) was degassed and backfilled with nitrogen, repeat this process three times. Subsequently, degassed dioxane (20 mL) and water (20 mL) were added to dissolve the reaction mixture, which was then heated to reflux for 12 hours. Upon completion of the reaction, the mixture was extracted with ethyl acetate and water. The combined organic layers were dried over anhydrous $MgSO_4$ and concentrated under reduced pressure. The crude product was further purified by column chromatography (ethyl acetate/hexane = 1:5), yielding a yellow solid (850 mg, 92%). ^{1}H NMR (400 MHz, $CDCl_3$) δ 8.48-8.41 (m, 2H), 8.39-8.32 (m, 2H), 7.75-7.66 (m, 2H), 7.66-7.57 (m, 2H), 3.17 (s, 3H). The observed NMR shifts are in agreement with literature values. [3]

2. Single crystals X-ray diffraction data
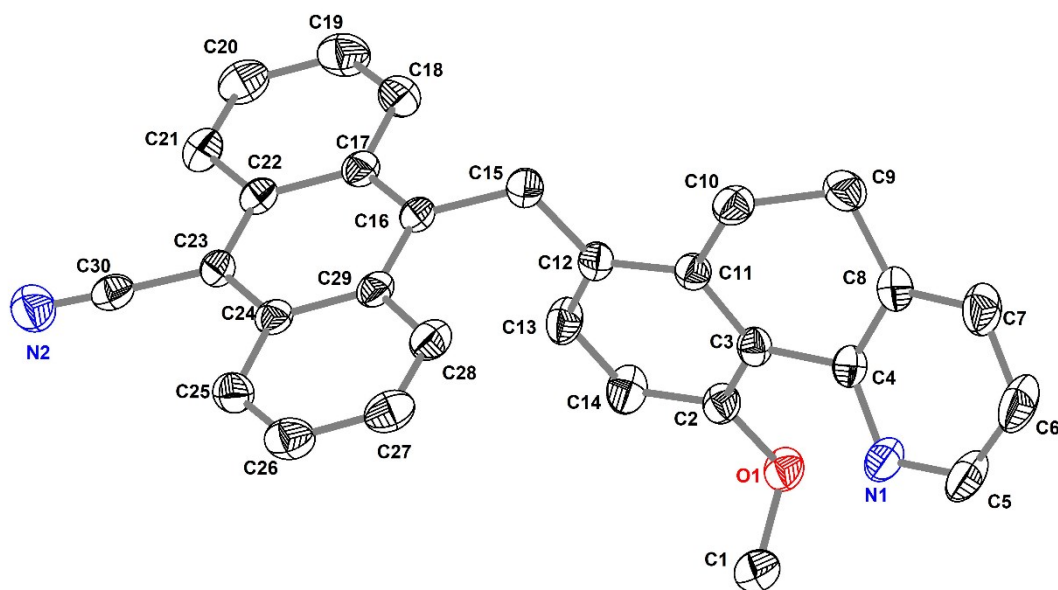
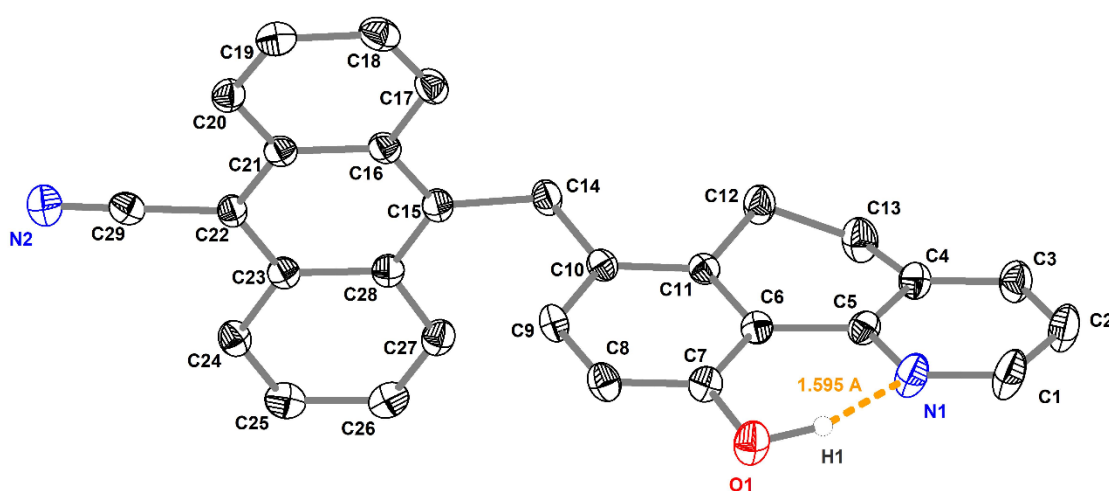**Fig. S1.** Structure of compound **7** with thermal ellipsoids shown at the 50 % probability level, the hydrogen atoms are omitted. CCDC Number: 2421278

Empirical formula	C30H22N2O
Formula weight	426.49
Temperature	200(2) K
Wavelength	0.71073 Å
Crystal system	Monoclinic
Space group	P 21/n
Unit cell dimensions	a = 9.2331(3) Å a= 90°.
	b = 7.8326(3) Å b= 93.4080(10)°.
	c = 29.3232(12) Å g = 90°.
Volume	2116.88(14) Å^3
Z	4
Density (calculated)	1.338 Mg/m^3
Absorption coefficient	0.081 mm^{-1}
F(000)	896
Crystal size	0.560 x 0.170 x 0.030 mm^3
Theta range for data collection	2.356 to 25.041°.
Index ranges	-10<=h<=10, -9<=k<=9, -34<=l<=34
Reflections collected	23366
Independent reflections	3734 [R(int) = 0.0697]

Completeness to theta = 25.041°	99.6 %
Refinement method	Full-matrix least-squares on F^2
Data / restraints / parameters	3734 / 0 / 299
Goodness-of-fit on F^2	1.017
Final R indices [I>2sigma(I)]	R1 = 0.0409, wR2 = 0.1109
R indices (all data)	R1 = 0.0523, wR2 = 0.1190
Extinction coefficient	n/a
Largest diff. peak and hole	0.173 and -0.190 e.Å^{-3}

Fig. S2. Structure of compound **8** with thermal ellipsoids shown at the 50 % probability level. The hydrogen atoms, except for H1, are omitted. CCDC Number: 2421279

Empirical formula	C29H20N2O	
Formula weight	412.47	
Crystal system	Monoclinic	
Space group	P2$_1$/n	
Unit cell dimensions	a = 9.3731(7) Å	a= 90°.
	b = 8.0865(5) Å	b= 99.172(3)°.
	c = 26.5071(19) Å	g = 90°.
Volume	1983.4(2) Å^3	
Z	4	
F(000)	864	
Density (calculated)	1.381 Mg/m^3	
Wavelength	1.54178 Å	
Cell parameters reflections used	9939	

Theta range for Cell parameters 3.38 to 70.16°.

Absorption coefficient 0.660 mm^{-1}

Temperature 100(2) K

Crystal size 0.100 x 0.100 x 0.050 mm^3

Data collection

Diffractometer Bruker AXS D8 VENTURE, PhotonIII_C28

Absorption correction Semi-empirical from equivalents

Max. and min. transmission 1.0000 and 0.8555

No. of measured reflections 26255

No. of independent reflections 3734 [R(int) = 0.0503]

No. of observed [I>2_igma(I)] 3418

Completeness to theta = 67.679° 99.6 %

Theta range for data collection 3.378 to 70.151°.

Refinement

Final R indices [I>2sigma(I)] R1 = 0.0452, wR2 = 0.1215

R indices (all data) R1 = 0.0487, wR2 = 0.1257

Goodness-of-fit on F^2 1.007

No. of reflections 3734

No. of parameters 293

No. of restraints 0

Largest diff. peak and hole 0.754 and -0.348 e.Å^{-3}

3. NMR spectra
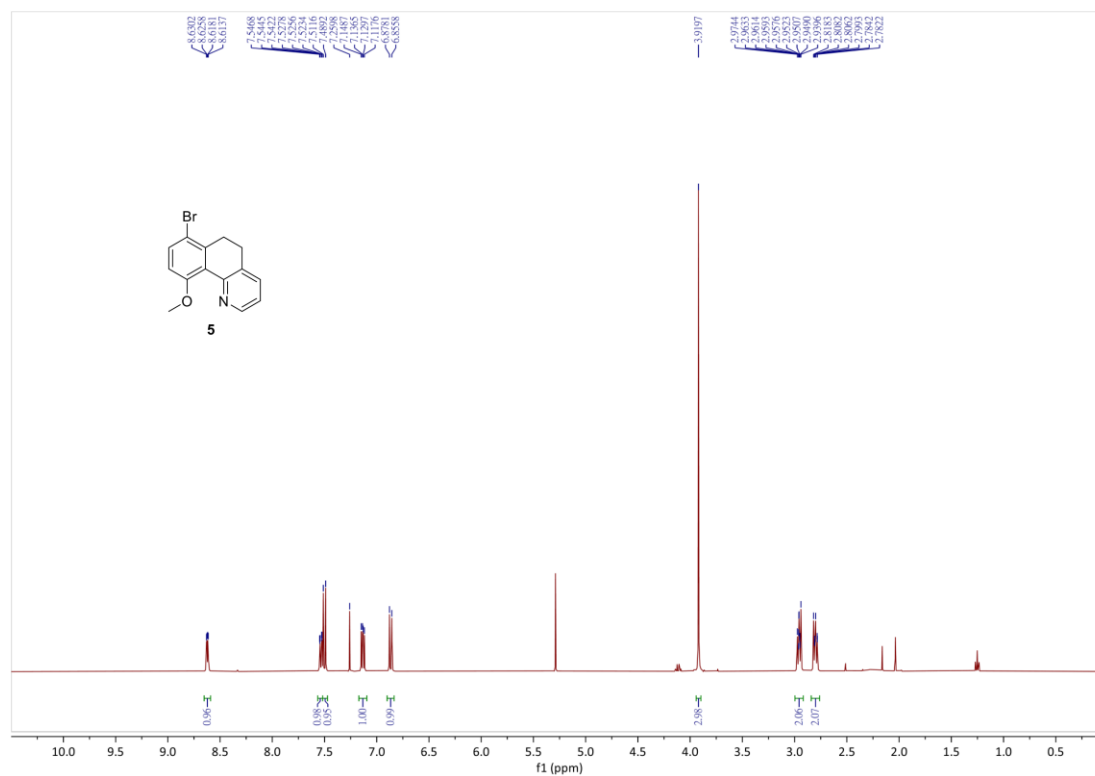
Fig. S3. ^{1}H NMR (400 MHz) of compound **5** in CDCl$_3$
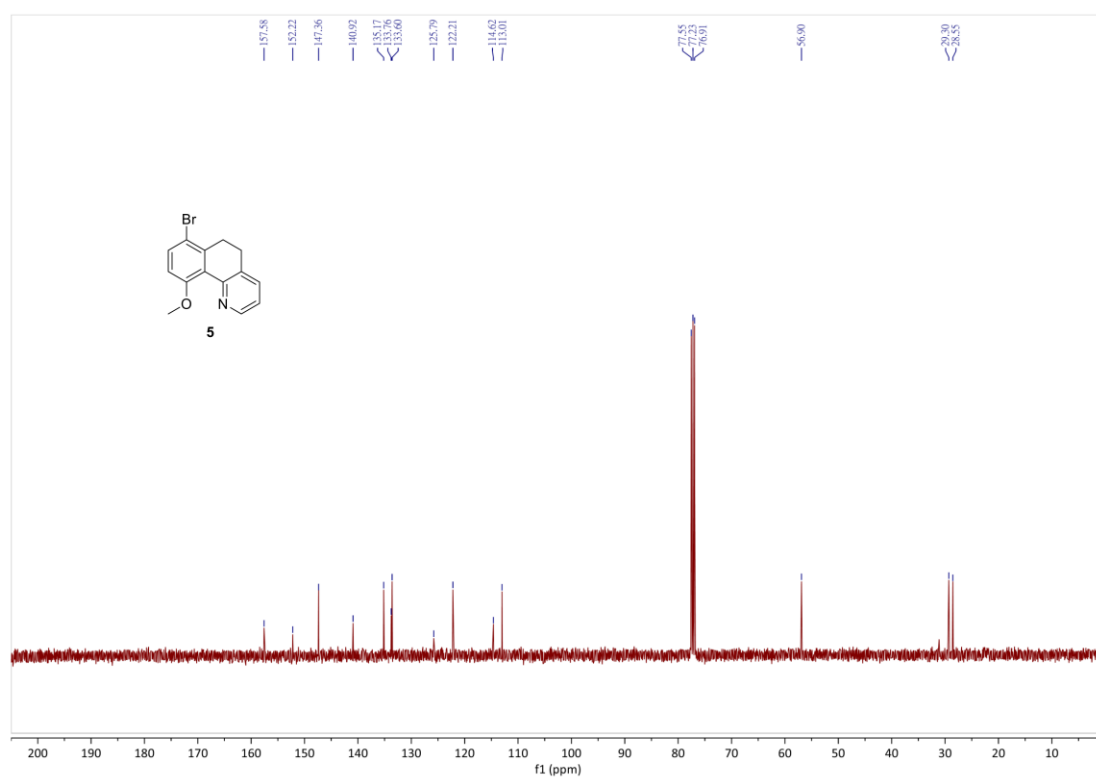
Fig. S4. ^{13}C NMR (100.6 MHz) of compound **5** in CDCl$_3$
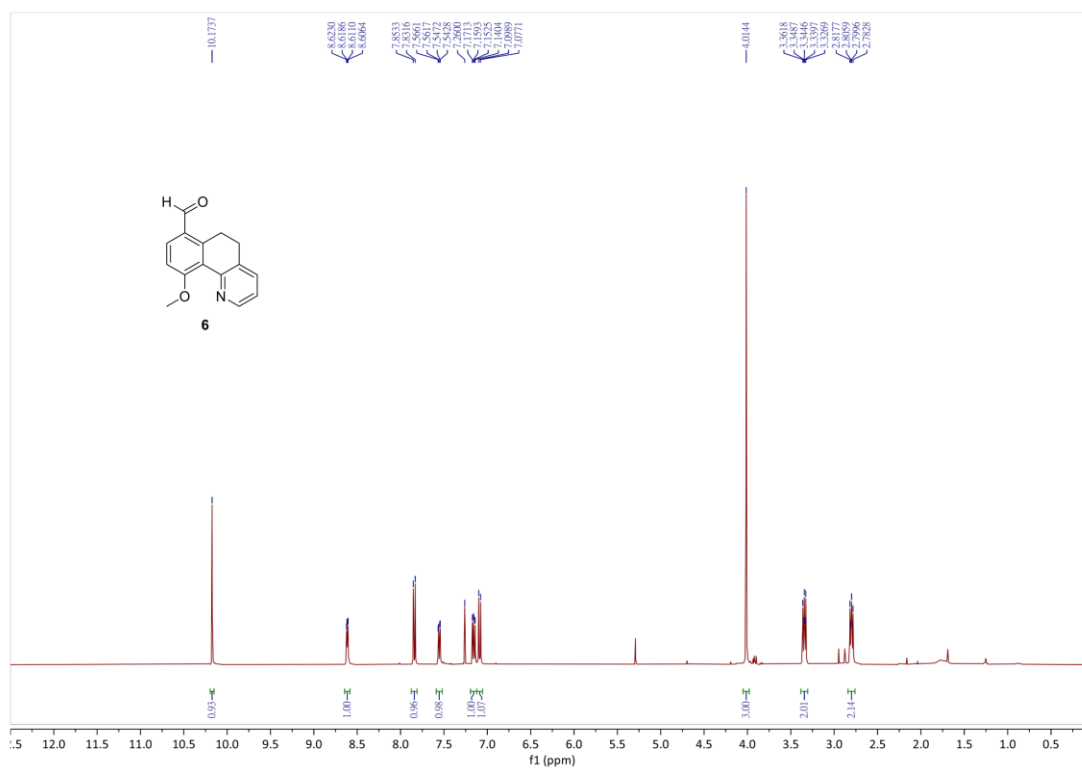
Fig. S5. ^{1}H NMR (400 MHz) of compound **6** in CDCl$_3$
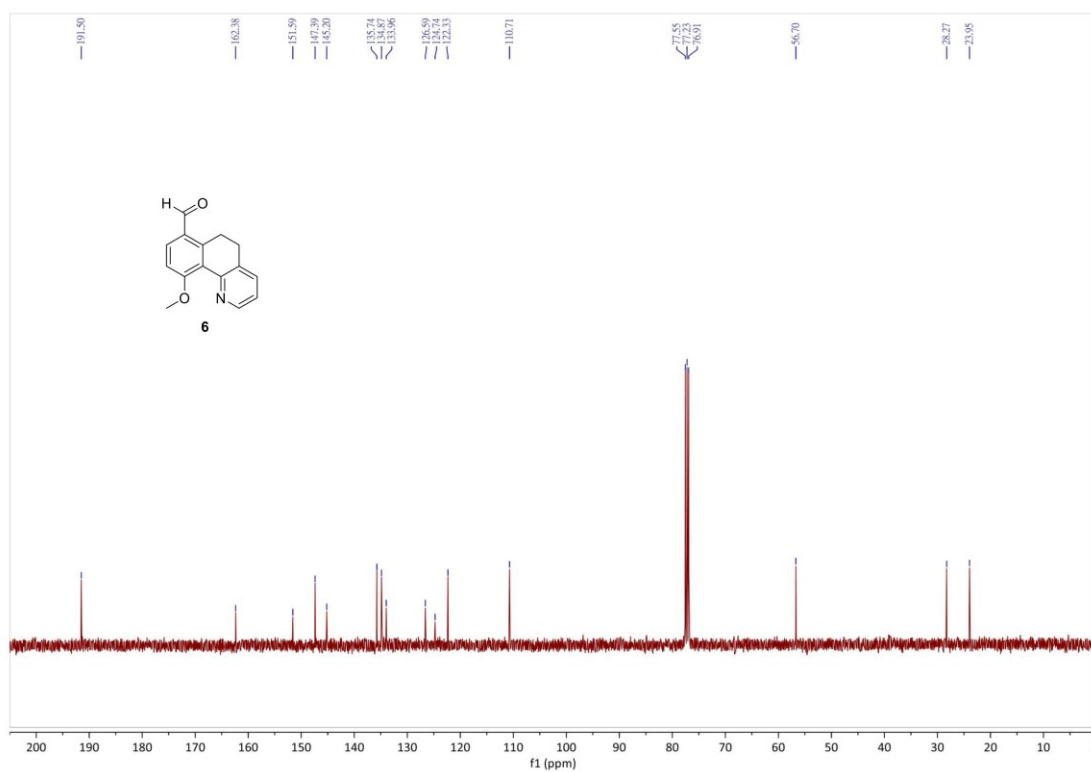
Fig. S6. ^{13}C NMR (100.6 MHz) of compound **6** in CDCl$_3$

Fig. S7. ^{1}H NMR (400 MHz) of compound **7** in DMSO-d$_6$

Fig. S8. ^{13}C NMR (100.6 MHz) of compound **7** in DMSO-d$_6$
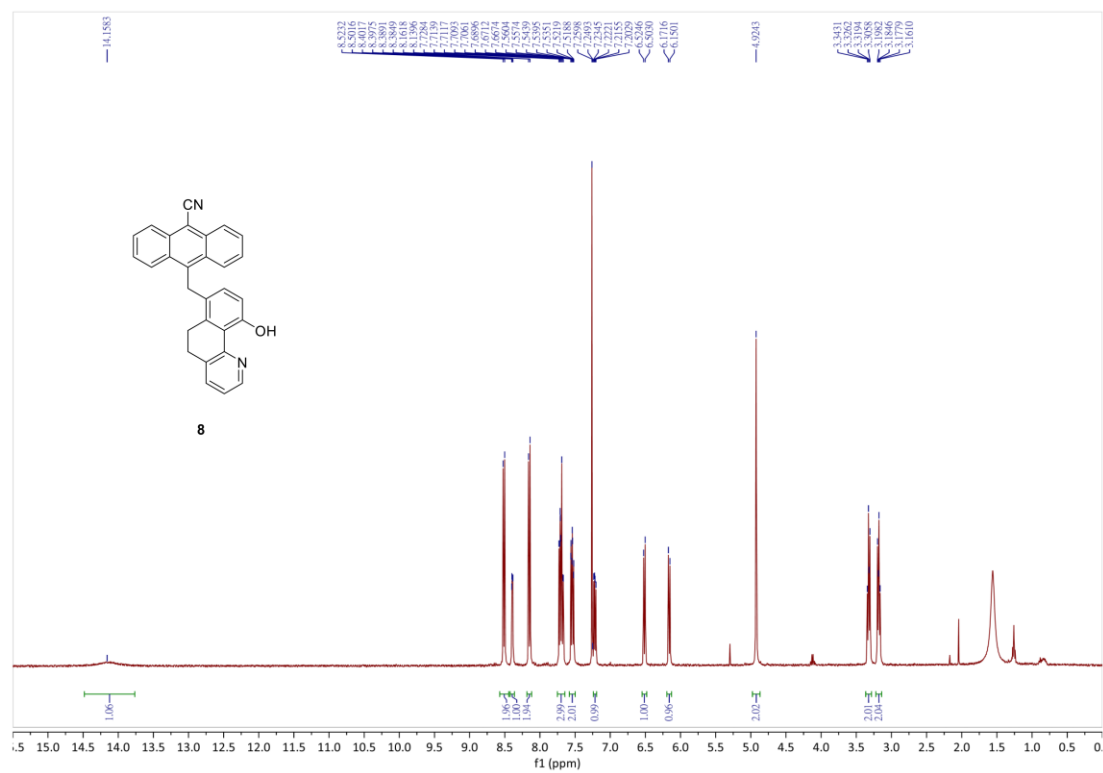
Fig. S9. ^{1}H NMR (400 MHz) of compound **8** in CDCl$_3$
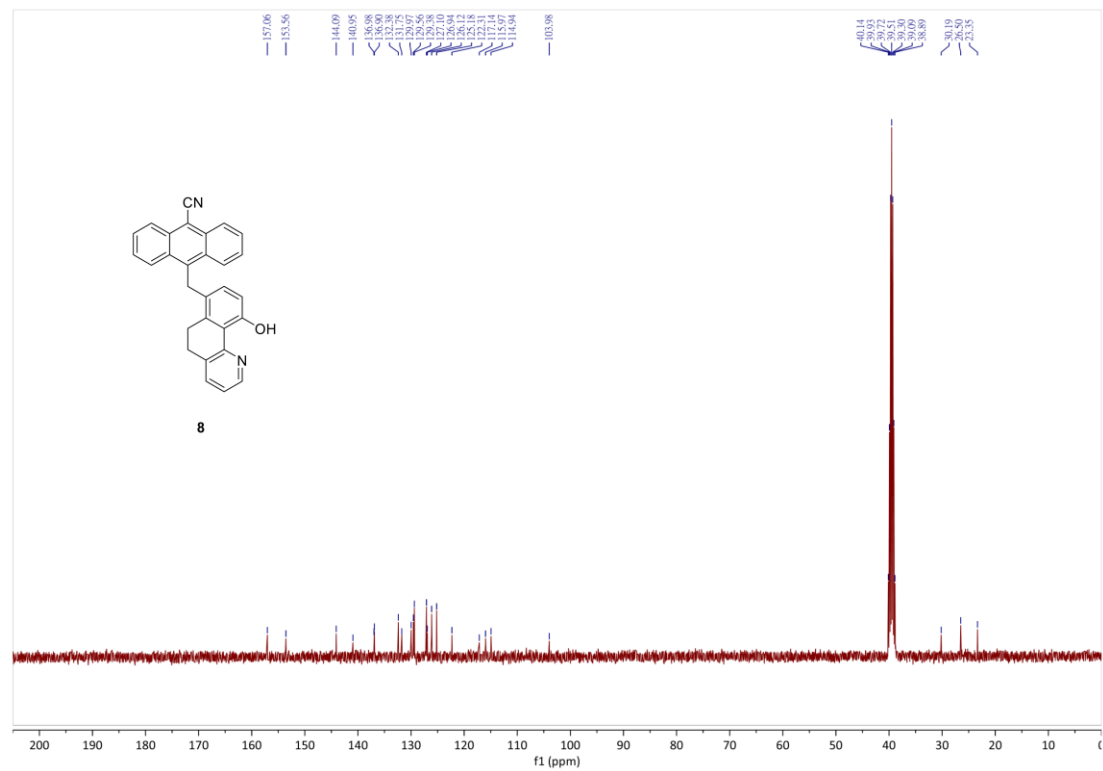
Fig. S10. ^{13}C NMR (100.6 MHz) of compound **8** in DMSO-d$_6$
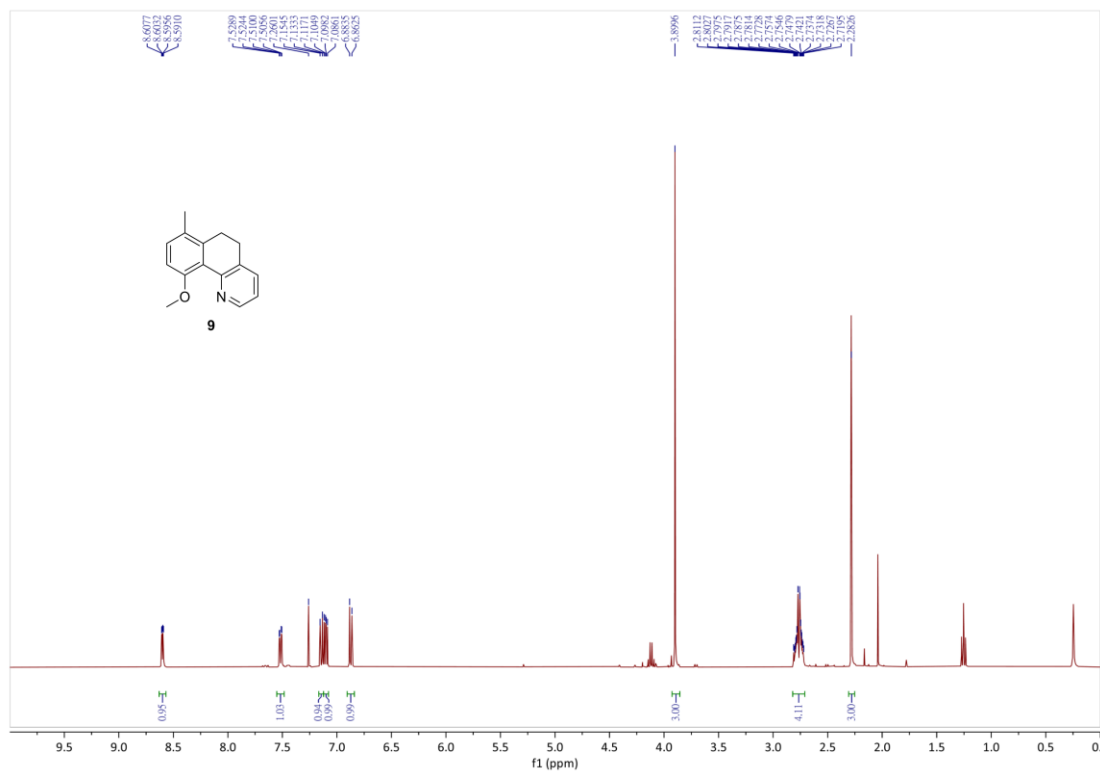
Fig. S11. ^{1}H NMR (400 MHz) of compound **9** in CDCl$_3$
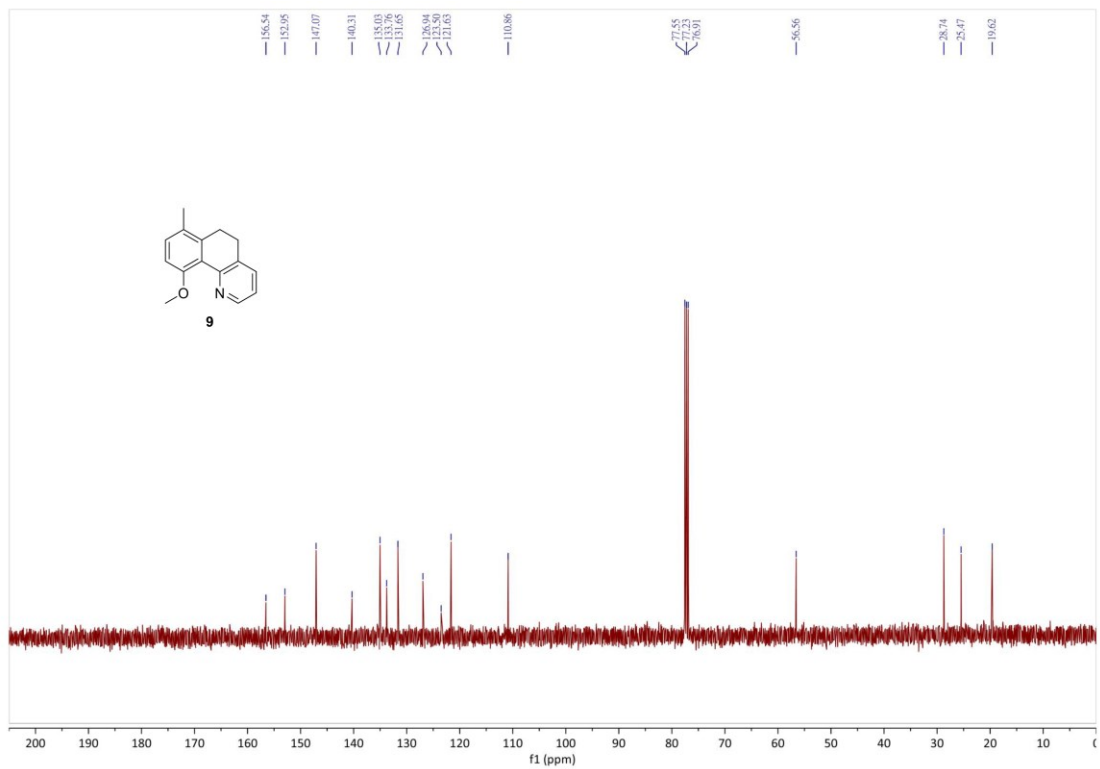
Fig. S12. ^{13}C NMR (100.6 MHz) of compound **9** in CDCl$_3$
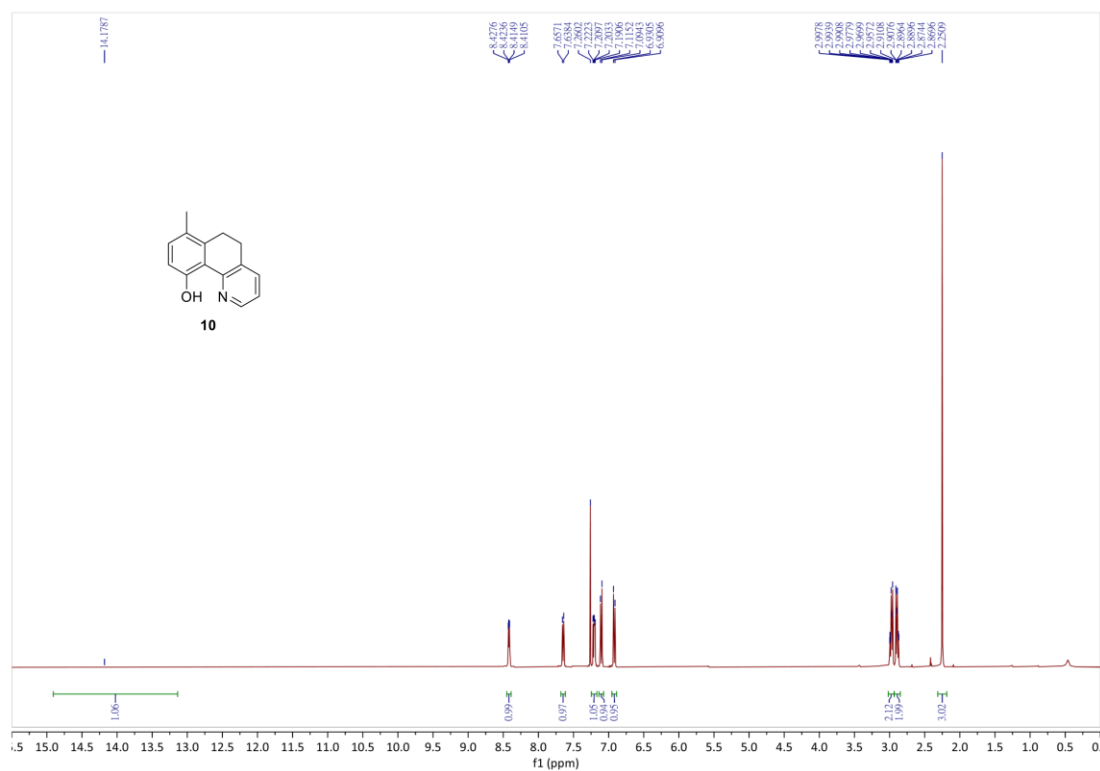
Fig. S13. ^{1}H NMR (400 MHz) of compound **10** in CDCl$_3$
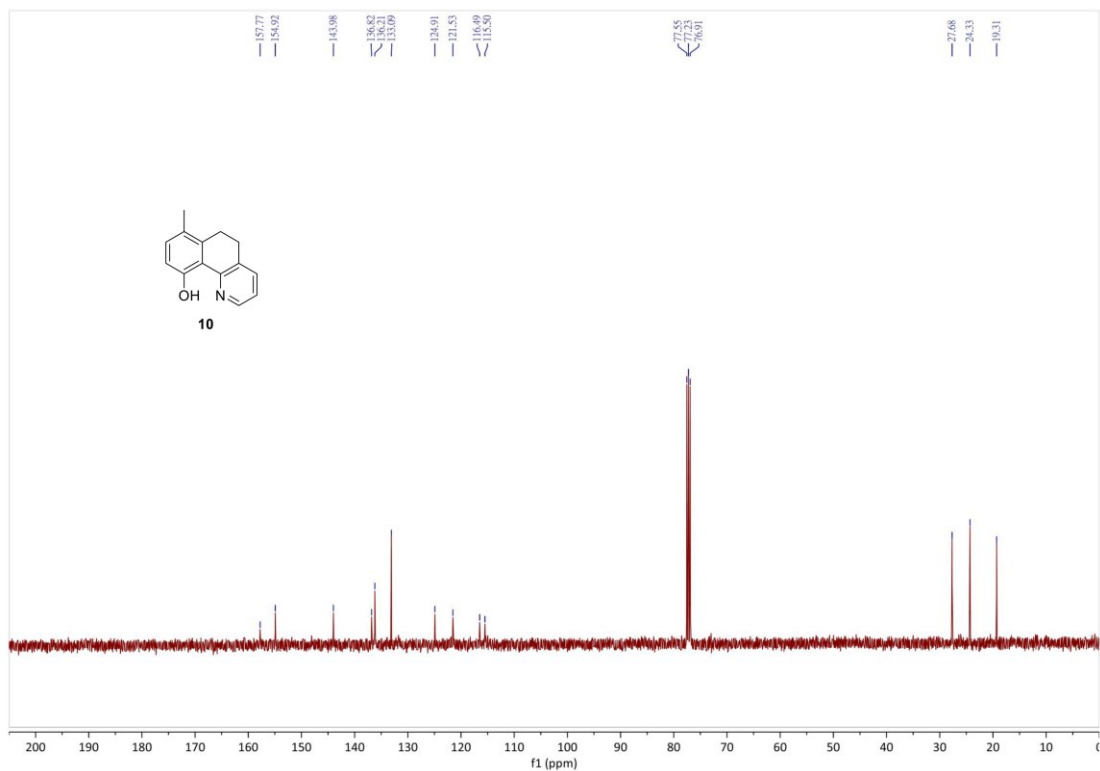
Fig. S14. ^{13}C NMR (100.6 MHz) of compound **10** in CDCl$_3$

4. Photophysical properties
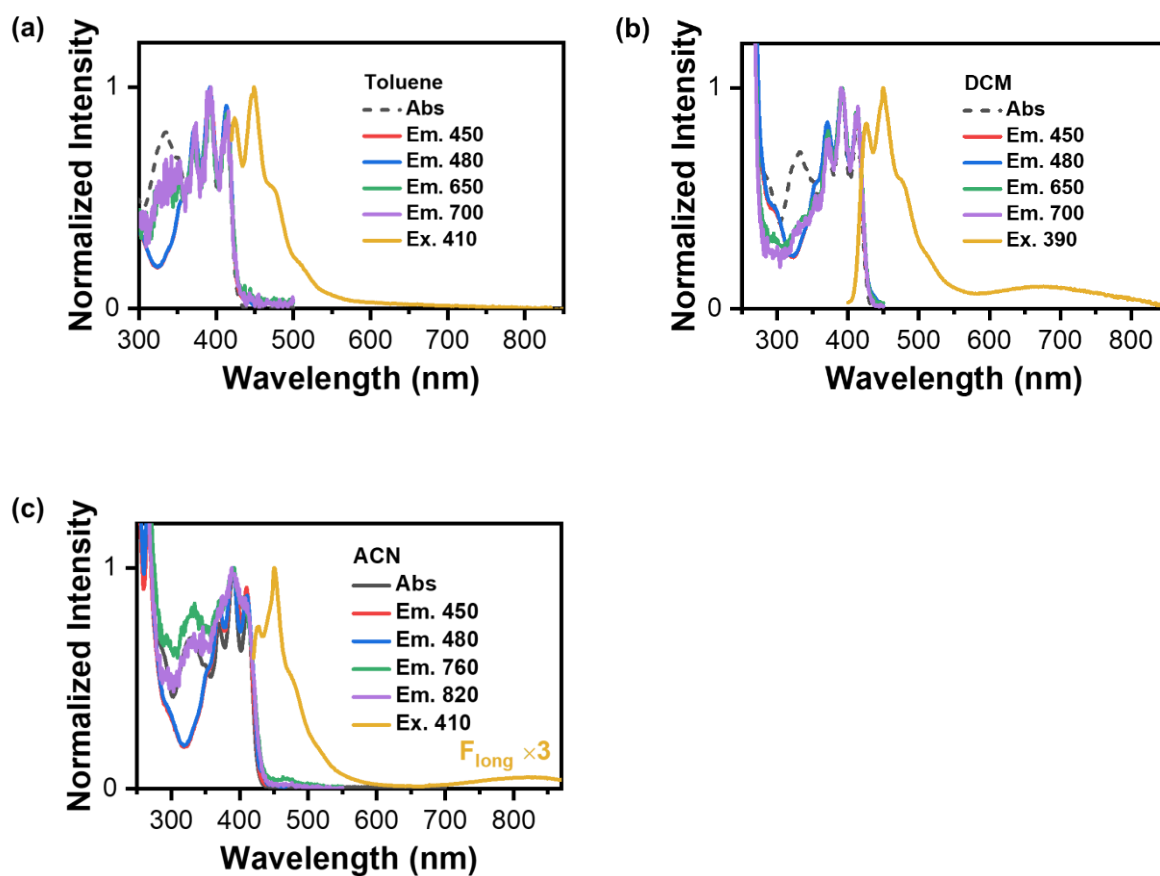
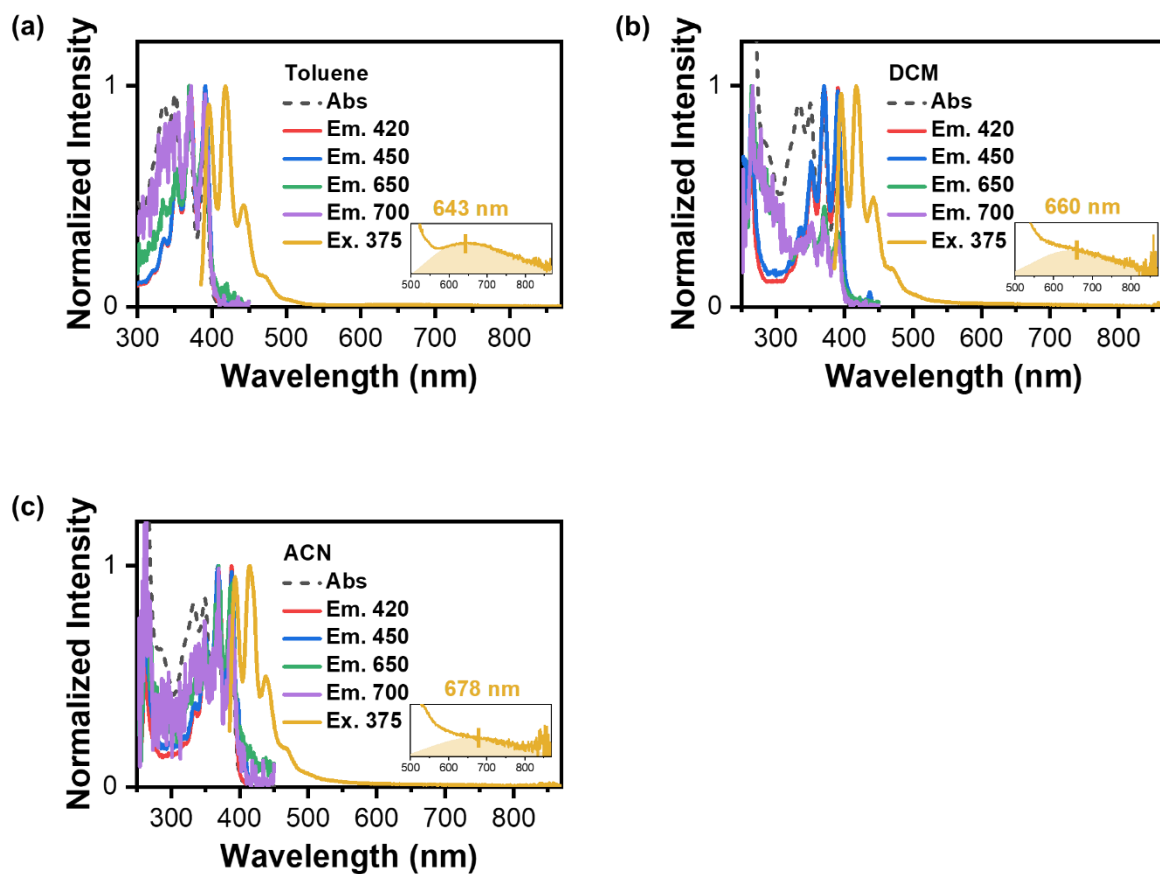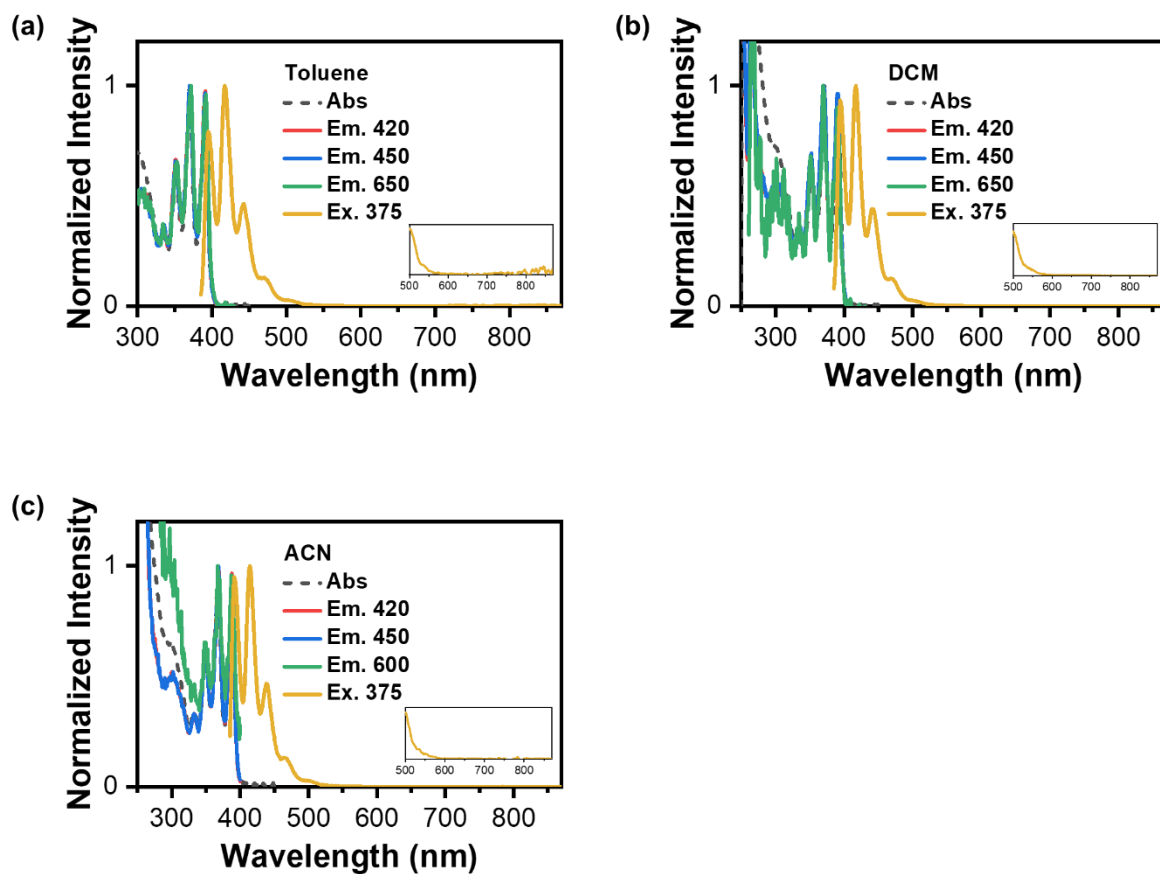**Fig. S15.** The steady-state absorption, excitation, and emission spectra of **triad 1** in (a) Toluene, (b) DCM, and (c) ACN at 298K. The term "Abs" corresponds to the absorption spectra, "Em" denotes the monitored wavelengths of emission, and "Ex" signifies the excitation wavelength utilized in the measurements.
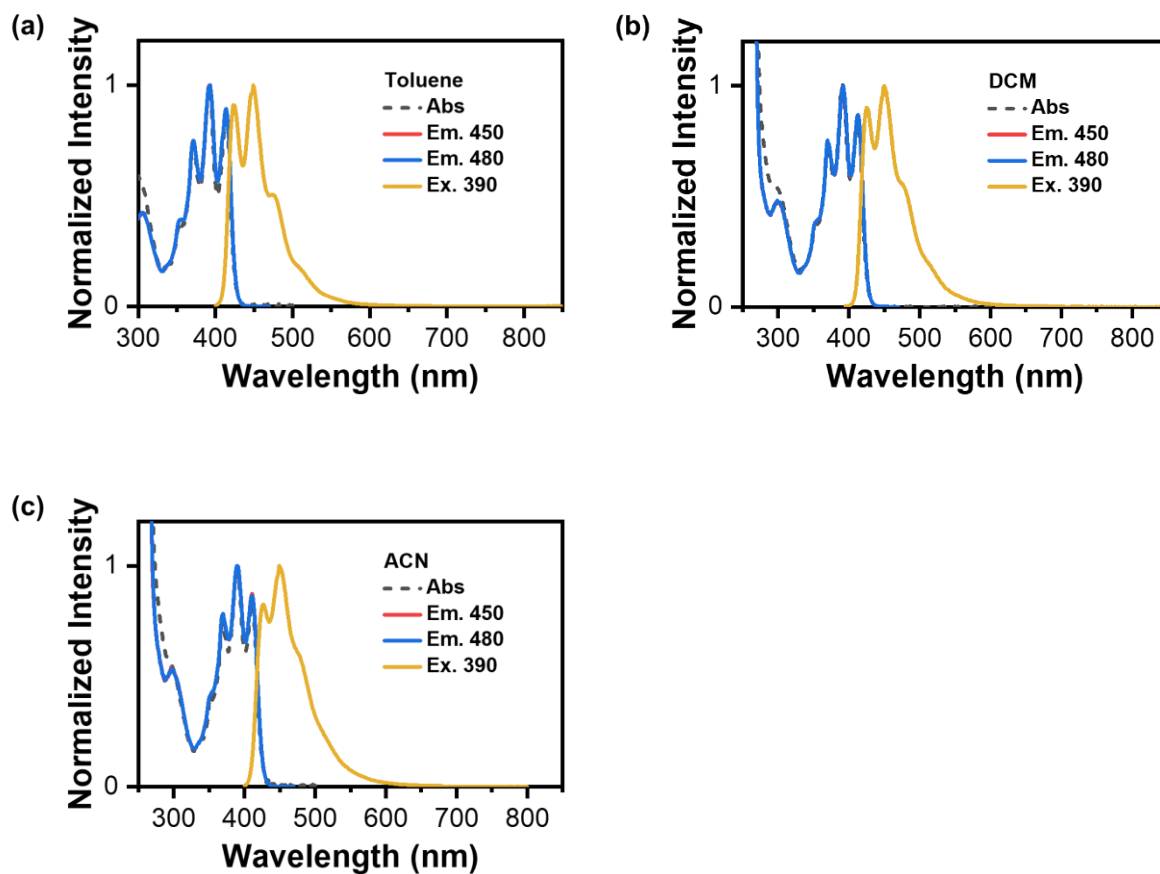
Fig. S16. The steady-state absorption, excitation, and emission spectra of **triad 1a** in (a) Toluene, (b) DCM, and (c) ACN at 298K.

Fig. S17. The steady-state absorption, excitation, and emission spectra of **triad 5** in (a) Toluene, (b) DCM, and (c) ACN at 298K.

Fig. S18. The steady-state absorption, excitation, and emission spectra of **triad 5a** in (a) Toluene, (b) DCM, and (c) ACN at 298K.
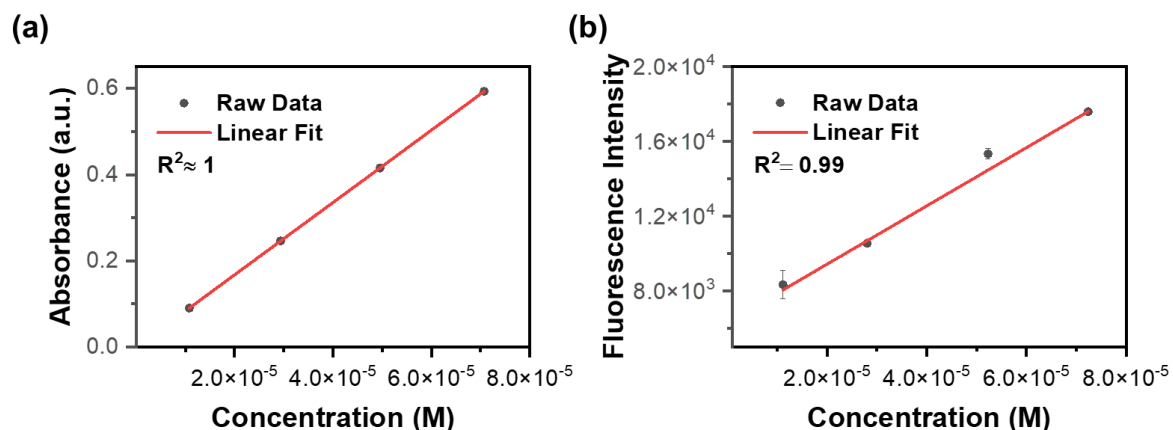
Fig. S19. Linear dependence between the concentration of triad 1 and (a) absorbance and (b) fluorescence intensity. Note that the fluorescence intensity is determined at the maximum F_{long} peak count. **Triad 1** is dissolved in ACN.
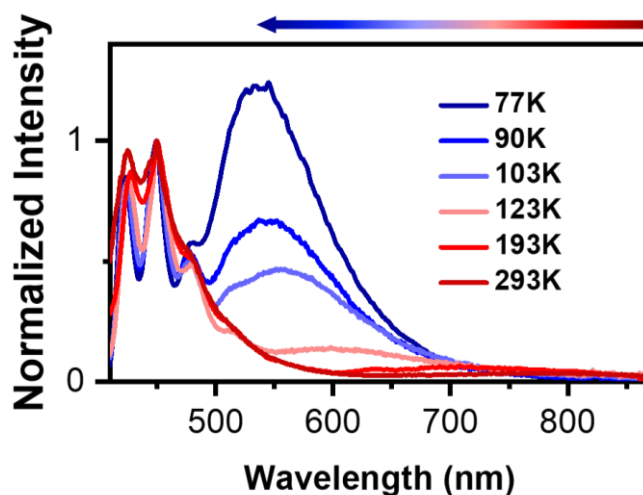

Fig. S20. The temperature-dependent steady-state emission spectra of **triad 1** in *n*-BuCN. The excitation wavelength is at 400 nm of the anthracene moiety to acquire the emission. The original short-wavelength anthracene-like emission has been concluded from the isomer of **triad 1**, for which the relaxation dynamic is independent of PCET[4]. The emission spectra are normalized at ~450 nm. For clarity, the arrow indicates the blueshift of the emission peak wavelength upon decreasing the temperature.

solvent	τ_{CSS} (ps)	k_{CSS} (s^{-1})
DCM	650	1.5×10^9
n-BuCN	71	1.4×10^{10}
ACN	33	3.1×10^{10}
DMF	30	3.4×10^{10}

Table S1. The pertinent lifetime fitting data of **triad 1** was recorded in different solvents, where k_{CSS} is the rate constant of CSS decay time. This experimental result is identical to the transient absorption measurements in the previous work.[5]
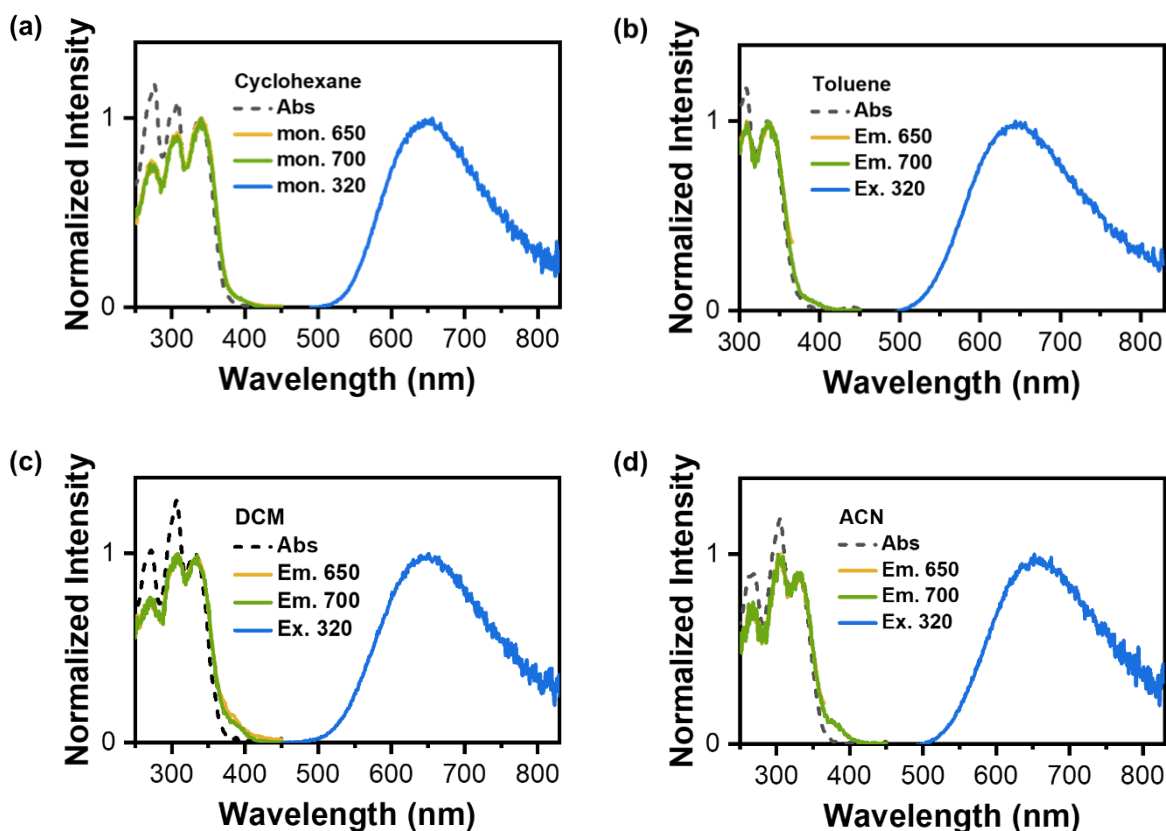
Fig. S21. The steady-state absorption, excitation, and emission spectra of **bPP** in (a) Cyclohexane, (b) Toluene, (c) DCM, and (d) ACN at 298K. The term "Abs" corresponds to the absorption spectra, "Em" denotes the monitored wavelengths of emission, and "Ex" signifies the excitation wavelength utilized in the measurements.
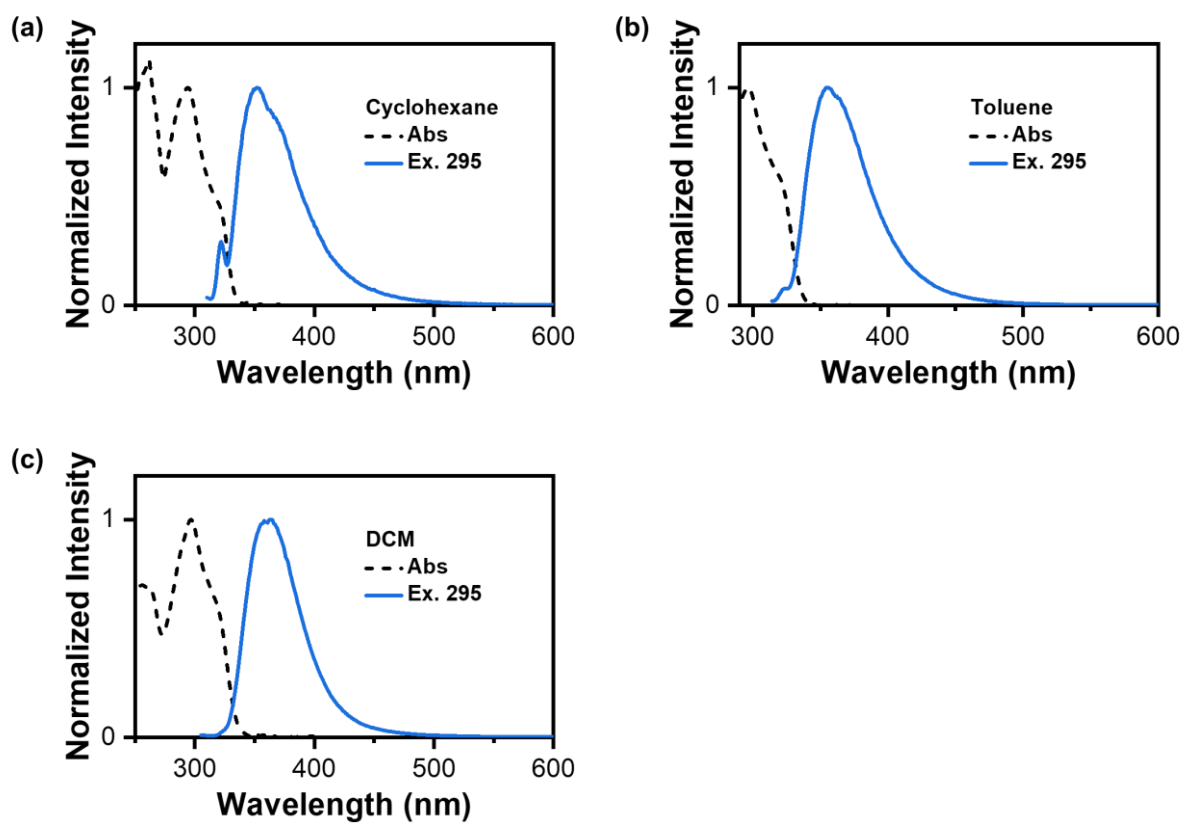
Fig. S22. The steady-state absorption, excitation, and emission spectra of **OMe-bPP** in (a) Cyclohexane, (b) Toluene, and (c) DCM at 298K.
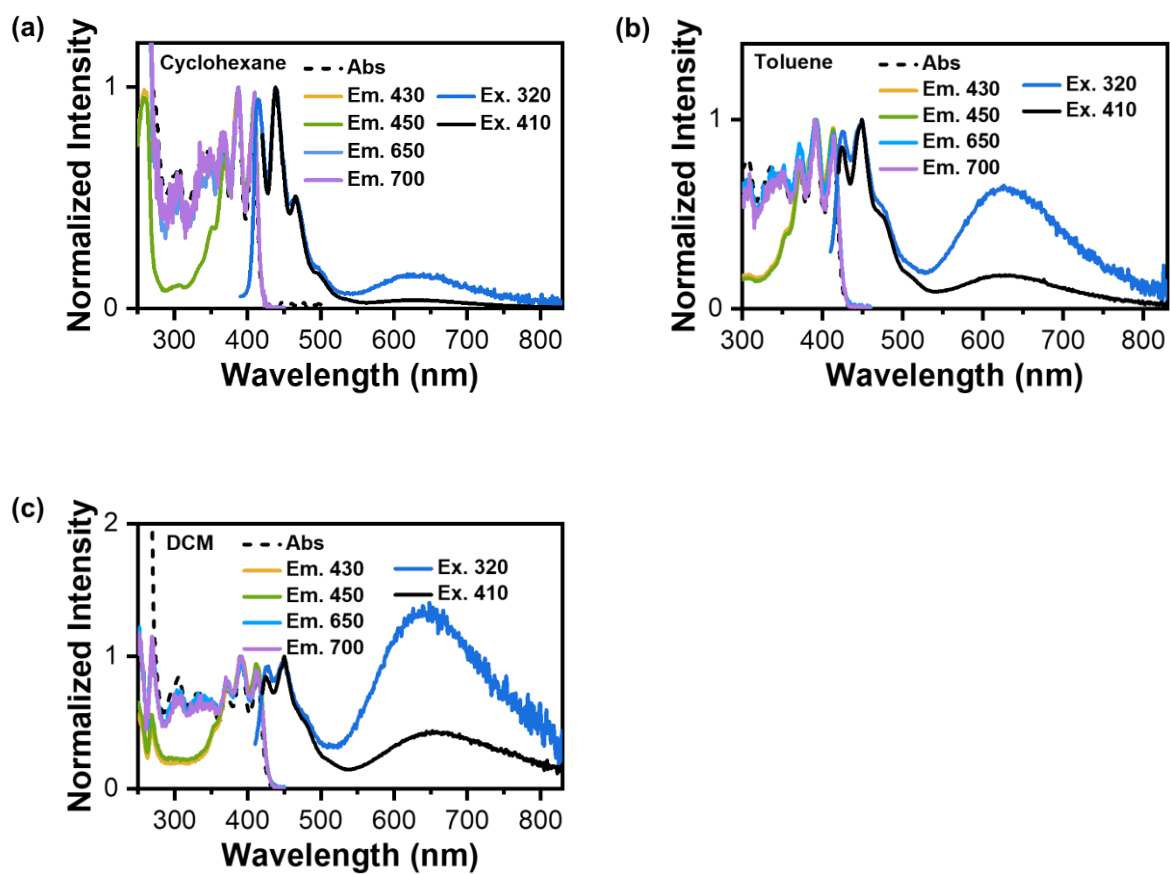
Fig. S23. The steady-state absorption, excitation, and emission spectra of **AbPP** in (a) Cyclohexane, (b) Toluene, and (c) DCM at 298K.
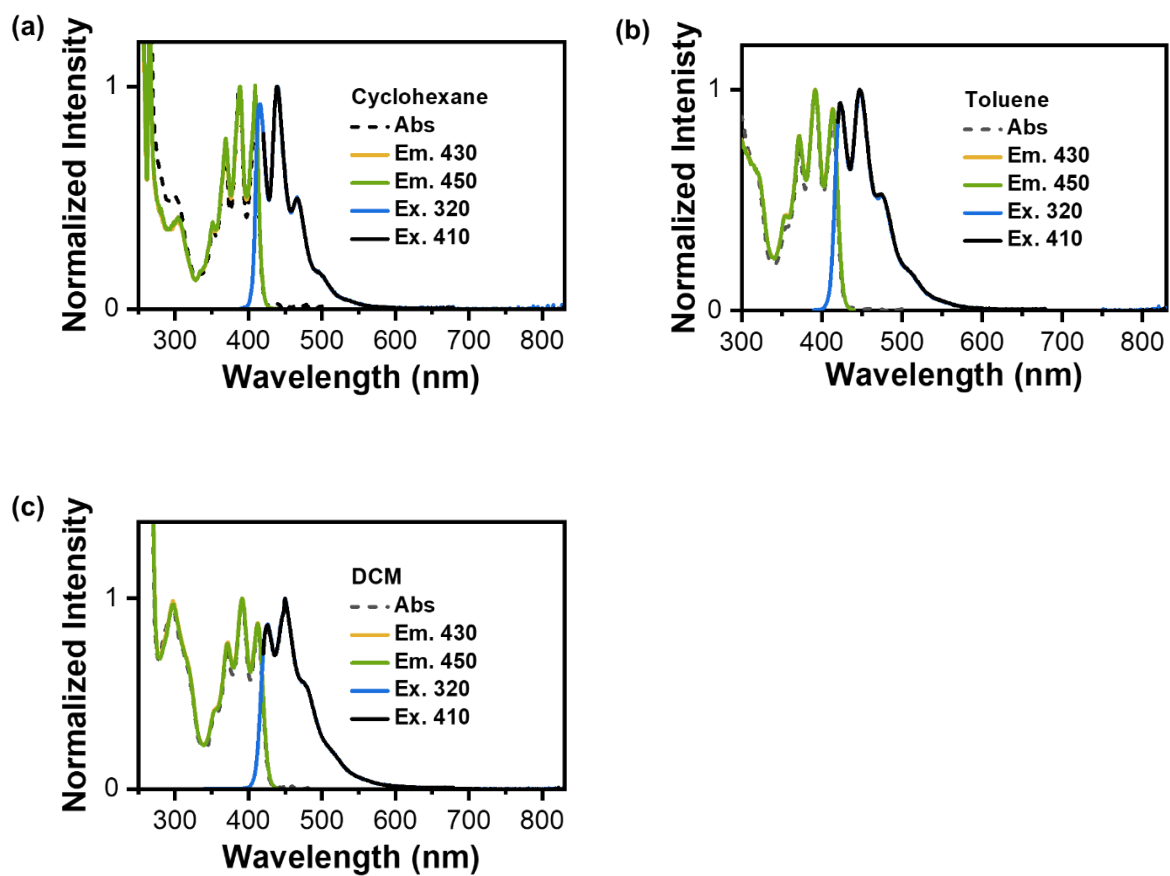
Fig. S24. The steady-state absorption, excitation, and emission spectra of **OMe-AbPP** in (a) Cyclohexane, (b) Toluene, and (c) DCM at 298K.
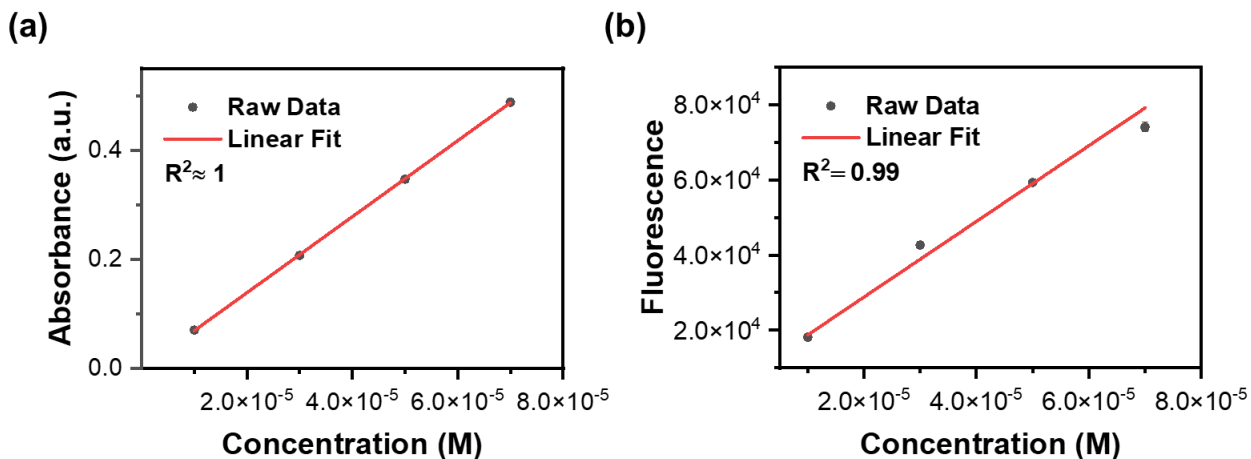
Fig. S25. Linear dependence between the concentration of **AbPP** and (a) absorbance and (b) fluorescence intensity. Note that the absorbance is determined at **320 nm**, and the fluorescence intensity, with an excitation wavelength of **320 nm**, is determined at the maximum F_{long} peak count. **AbPP** is dissolved in **TOL**.
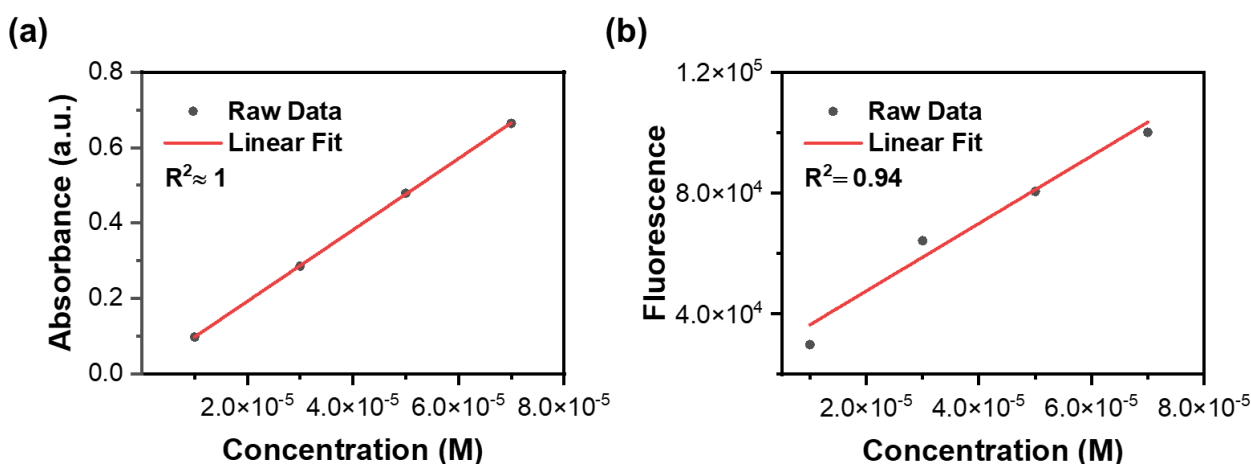

Fig. S26. Linear dependence between the concentration of **AbPP** and (a) absorbance and (b) fluorescence intensity. Note that the absorbance is determined at **410 nm**, and the fluorescence intensity, with an excitation wavelength of **410 nm**, is determined at the maximum F_{long} peak count. **AbPP** is dissolved in **TOL**.
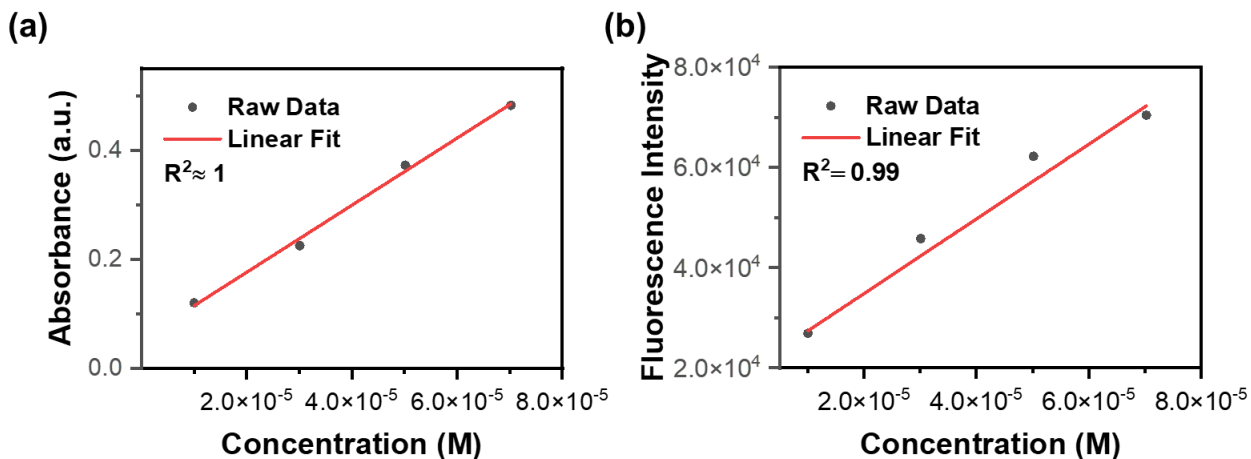
Fig. S27. Linear dependence between the concentration of **AbPP** and (a) absorbance and (b) fluorescence intensity. Note that the absorbance is determined at **320 nm**, and the fluorescence intensity, with an excitation wavelength of **320 nm**, is determined at the maximum F_{long} peak count. **AbPP** is dissolved in **DCM**.
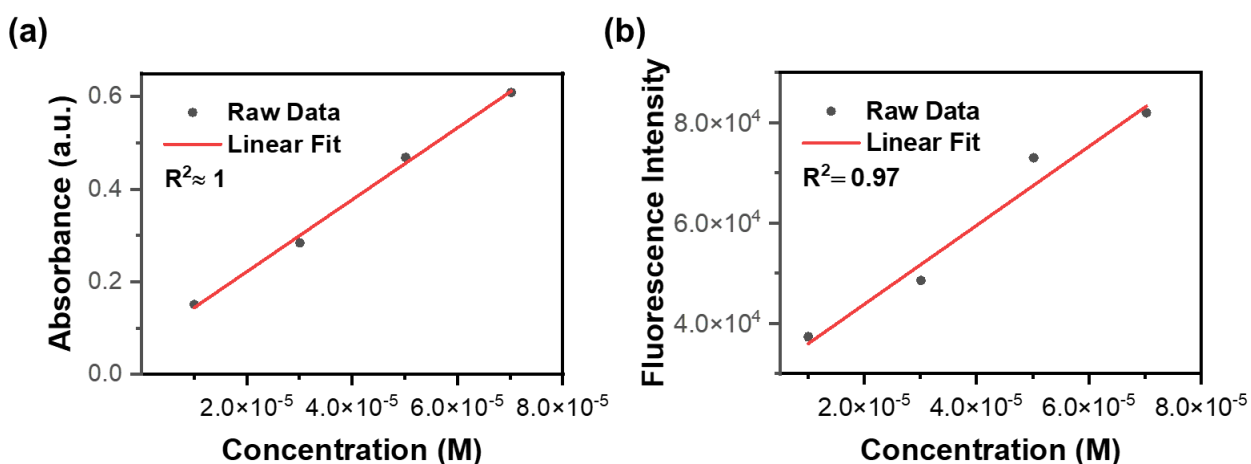

Fig. S28. Linear dependence between the concentration of **AbPP** and (a) absorbance and (b) fluorescence intensity. Note that the absorbance is determined at **410 nm**, and the fluorescence intensity, with an excitation wavelength of **410 nm**, is determined at the maximum F_{long} peak count. **AbPP** is dissolved in **DCM**.
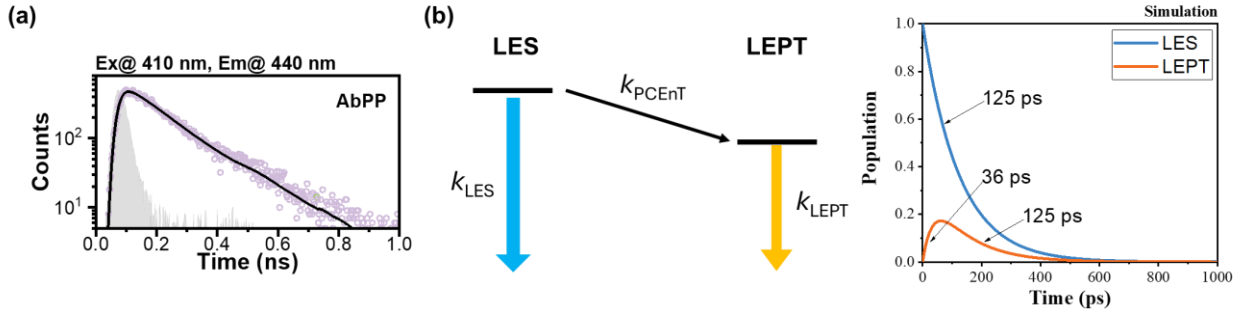
Fig. S29 (a) Excitation of **AbPP** in cyclohexane at 410 nm, showing a fast decay (~125 ps) due to PCEnT of the **CN-Ant** unit (monitored at 440 nm). (b) Kinetic model and simulation of the LES-to-LEPT population transfer in a nonpolar solvent.

Simulation of the inverted rise/decay time of AbPP in cyclohexane

In a nonpolar solvent such as cyclohexane, the kinetic concentration equations can be expressed as follows:

$$\frac{d[LES]}{dt} = -(k_{LES} + k_{PCEnT}\,[LES]) \qquad (1)$$

$$\frac{d[LEPT]}{dt} = k_{PCEnT}[LES] - k_{LEPT}[LEPT] \qquad (2)$$

$$[LES](t) = [LES]_0 \cdot \exp\left(-(k_{PCEnT} + k_{LES})t\right) \qquad (3)$$

where k_{PCEnT} is the rate constant of PCEnT from LES to LEPT, and k_{LES} and k_{LEPT} are the rate constant for LES and LEPT population decay, respectively. The PCEnT rate of **AbPP** was determined by monitoring the **CN-Ant** unit emission at 440 nm upon excitation at 410 nm. A sub-nanosecond decay time of 125 ps was observed (Fig. S29(a)), which is relatively slower than the tautomer emission decay (36 ps) observed from directly excited **bPP** (Fig. 1C). To further analyze this process, we performed a kinetic simulation to visualize the expected kinetic profiles, using input values of $k_{PCEnT} = 8 \times 10^9$ s-1 (125 ps) and $k_{LEPT} = 2.8 \times 10^{10}$ s^{-1} (36 ps). The calculation process is as follows.

Substituting Equation *(3)* into Equation *(2)*

$$\frac{d[LEPT]}{dt} + k_{LEPT}[LEPT](t) = k_{PCEnT}[LES]_0 \cdot \exp\left(-(k_{PCEnT} + k_{LES})t\right)$$

$$\exp(k_{LEPT})t \cdot \frac{d[LEPT]}{dt} + k_{LEPT}[LEPT](t) = k_{PCEnT}[LES]_0 \cdot \exp\left(k_{LEPT} - (k_{PCEnT} + k_{LES})t\right)$$

$$\frac{d}{dt}\left((\exp(k_{LEPT})t \cdot [LEPT](t)\right) = k_{PCEnT}[LES]_0 \cdot \exp\left((k_{LEPT} - (k_{PCEnT} + k_{LES}))t\right)$$

$$\int d(\exp(k_{LEPT})t \cdot [LEPT](t)) = \int k_{PCEnT}[LES]_0 \cdot \exp\left((k_{LEPT} - (k_{PCEnT} + k_{LES}))t\right)\,dt$$

$$\exp(k_{LEPT})t \cdot [LEPT](t) = k_{PCEnT}[LES]_0 \frac{\exp((k_{LEPT}-(k_{PCEnT}+k_{LES}))t)}{k_{LEPT}-(k_{PCEnT}+k_{LES})} + C \qquad (4)$$

For t = 0,

$$C = -\frac{k_{PCEnT}[LES]_0}{k_{LEPT}-(k_{PCEnT}+k_{LES})}$$

Substitute constant C back into equation *(4)*

$$[LEPT](t)$$
$$= \frac{k_{PCEnT}[LES]_0}{(k_{LES}+k_{PCEnT})-k_{LEPT}} \cdot \exp(-k_{LEPT}t) - \frac{k_{PCEnT}[LES]_0}{(k_{LES}+k_{PCEnT})-k_{LEPT}} \cdot \exp(-(k_{LES}+k_{PCEnT})t)$$

The simulation results, shown above, indicate that the LEPT population exhibits a 36 ps rise time followed by a 125 ps decay, matching the experimental results presented in Fig. 1D. When monitoring the LEPT emission band at 670 nm, the kinetic derivation clearly reveals that the faster decay appears as the rising component, while the slower PCEnT process corresponds to the decay component.

		LES	LEPT / CSS		
Solvent	monitor@	τ_{decay}(ps)	τ_{rise}(ps)	$\tau_{decay\ 1}$ (ps)	$\tau_{decay\ 2}$ (ps)
Cyclohexane[a]	440 nm	125	-	-	-
	600 nm		45	130	-
	650 nm		41	134	-
	700 nm		36	136	-
Toluene[b]	440 nm	31.8	-	-	-
	600 nm		35.4	35.7 (0.9996)	723.4 (0.0004)
	650 nm		36.1	36.9 (0.9994)	725.9 (0.0006)
	700 nm		36.4	37.6 (0.9992)	735.4 (0.0008)
DCM[a, b]	440 nm	7.5[b]	-	-	-
	600 nm		2.1[b]	38 (0.83)[a]	438 (0.17)[a]
	650 nm		5.3[b]	39 (0.75)[a]	426 (0.25)[a]
	700 nm		7.3[b]	40 (0.70)[a]	443 (0.30)[a]
D7A1[a, b]	440 nm	5.8[b]	-	-	-
	600 nm		1.5[b]	33 (0.95)[a]	227 (0.05)[a]
	650 nm		3.3[b]	34 (0.88)[a]	203 (0.12)[a]
	700 nm		4.2[b]	35 (0.81)[a]	208 (0.19)[a]
ACN[a, c]	440 nm	2.8[c]	-	-	-
	600 nm		2.8[b]	27[a]	
	650 nm		3.2[b]	28[a]	26.4[c]
	700 nm		3.2[b]	33[a]	

Table S2. Lifetime fitting data of **AbPP** was recorded in different solvents with 410 nm excitation. (The parentheses after data $\tau_{decay\ 1}$ and $\tau_{decay\ 2}$ indicate the pre-exponential factor.)
[a] Recorded by time-correlated single photon counting (TCSPC). [b] Recorded by upconversion.
[c] Recorded by femtosecond transient absorption (TA).
*D7A1 is mixture of DCM:ACN = 7:1 (v:v), D6A1 is mixture of DCM:ACN = 6:1 (v:v)

Solvent	τ_{decay} (ps)
Cyclohexane	36
Toluene	37
DCM	38
ACN	22

Table S3. Lifetime fitting data of **bPP** obtained using time-correlated single-photon counting (TCSPC) in different solvents under 300 nm excitation.
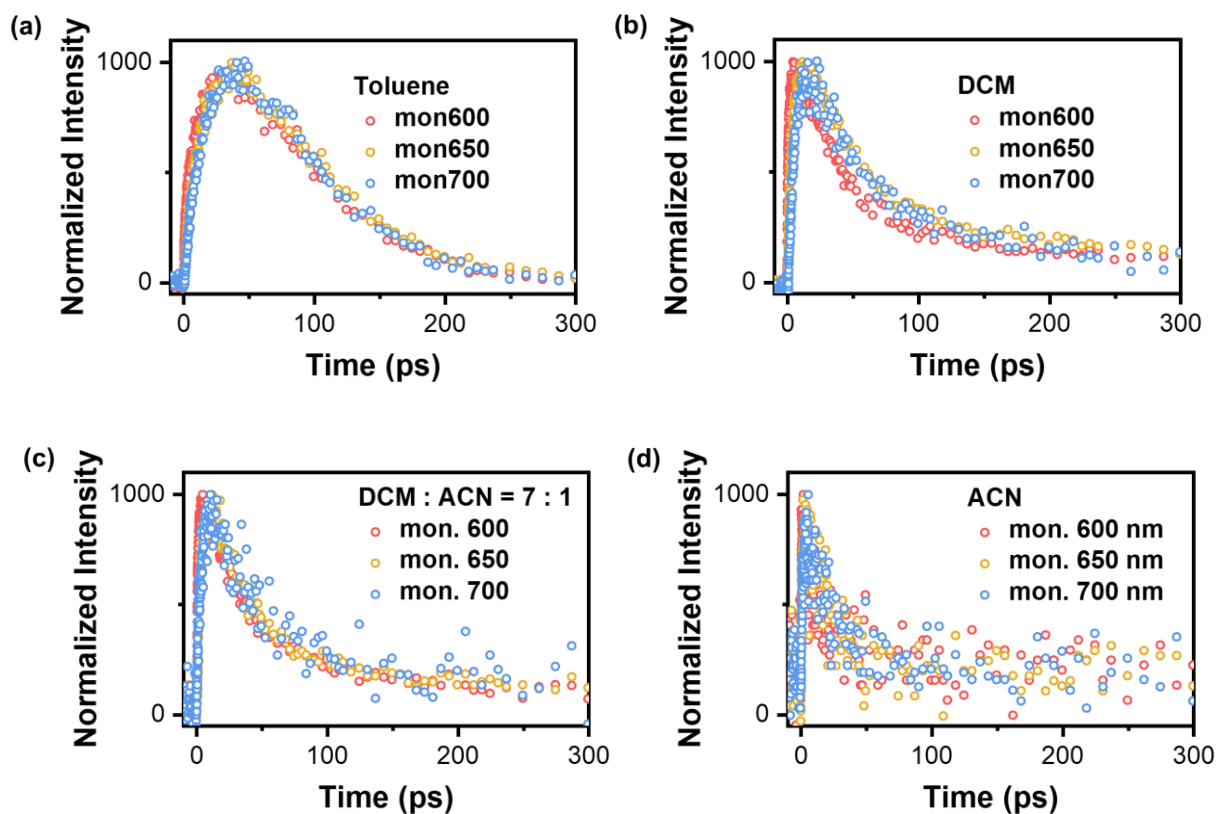
Fig. S30. The upconversion lifetime spectroscopy of **AbPP** in (a) Toluene, (b) DCM, (c) DCM:ACN=7:1 (v:v), and (d) ACN. The monitor wavelengths are set at 600 nm, 650 nm, and 700 nm in each solvent and the fitting lifetime data are summarized in **Table S2**.
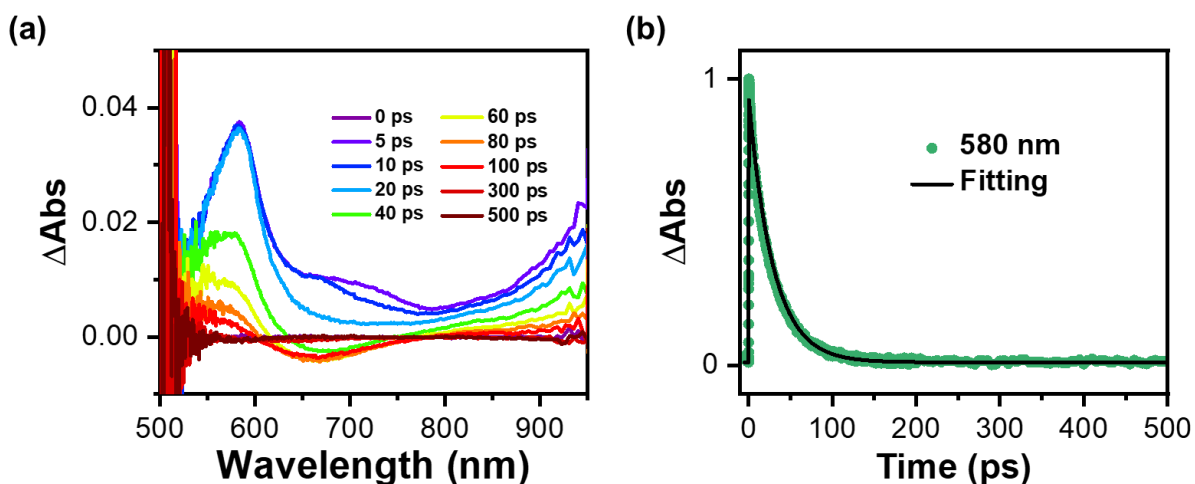

Fig. S31. Transient absorption data of **AbPP** in Toluene. (a) transient absorption spectra at various delay times. (b) time traces at a probe wavelength of 580 nm. The green data fitted to τ_{decay}=28.9 ps (decay of the LES and formation of the LEPT and CSS).
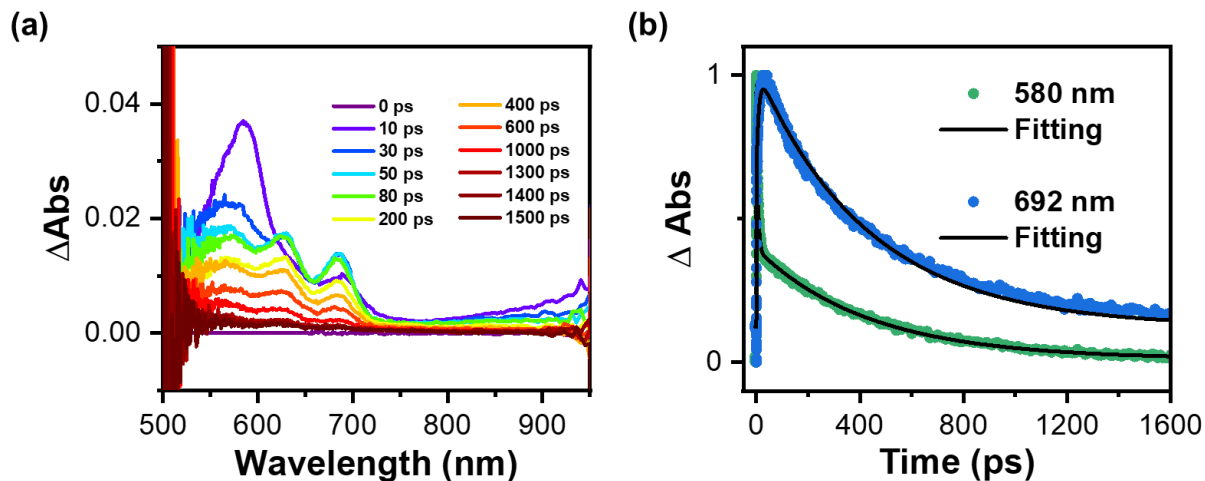
Fig. S32. Transient absorption data of **AbPP** in DCM. (a) transient absorption spectra at various delay times. (b) time traces at a probe wavelength of 580 nm and 692 nm. The green data fitted to τ_{decay}=5.3 ps (decay of the LES and formation of the CSS and LEPT) along with a long decay component attributed to the CSS decay due to spectral overlap between the LES and CSS. The blue data fitted to τ_{rise}=9.1 (rise of the CSS) and τ_{decay}=435.7 ps (decay of the CSS).
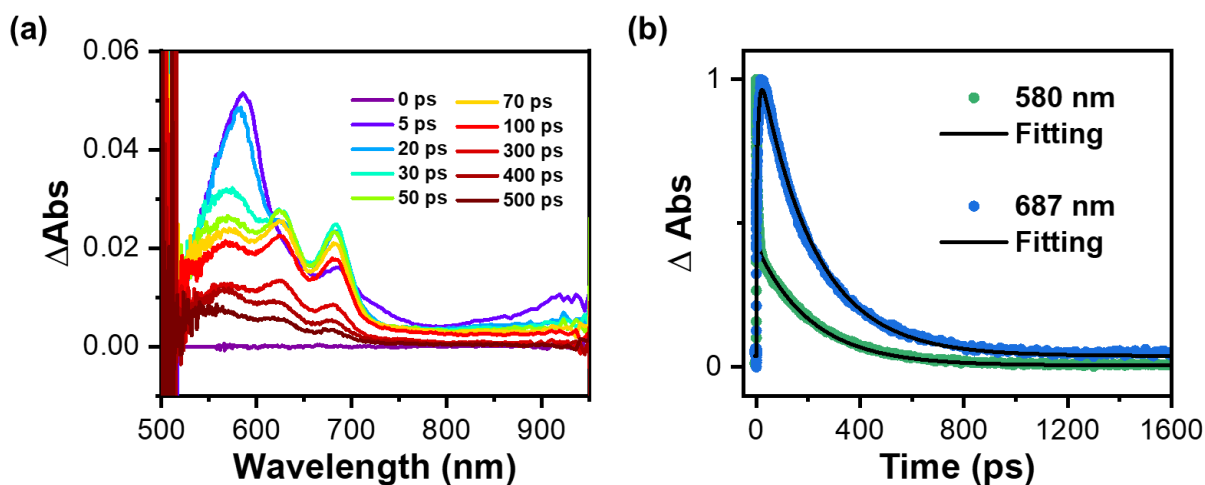

Fig. S33. Transient absorption data of **AbPP** in DCM:ACN=7:1 (v:v). (a) transient absorption spectra at various delay times. (b) time traces at various probe wavelengths. The green data fitted to τ_{decay}=3.7 ps (decay of the LES and formation of the CSS and LEPT) along with a long decay component attributed to the CSS decay due to spectral overlap between the LES and CSS. The blue data fitted to τ_{rise}=7.9 (rise of the CSS) and τ_{decay}=212.5 ps (decay of the CSS).
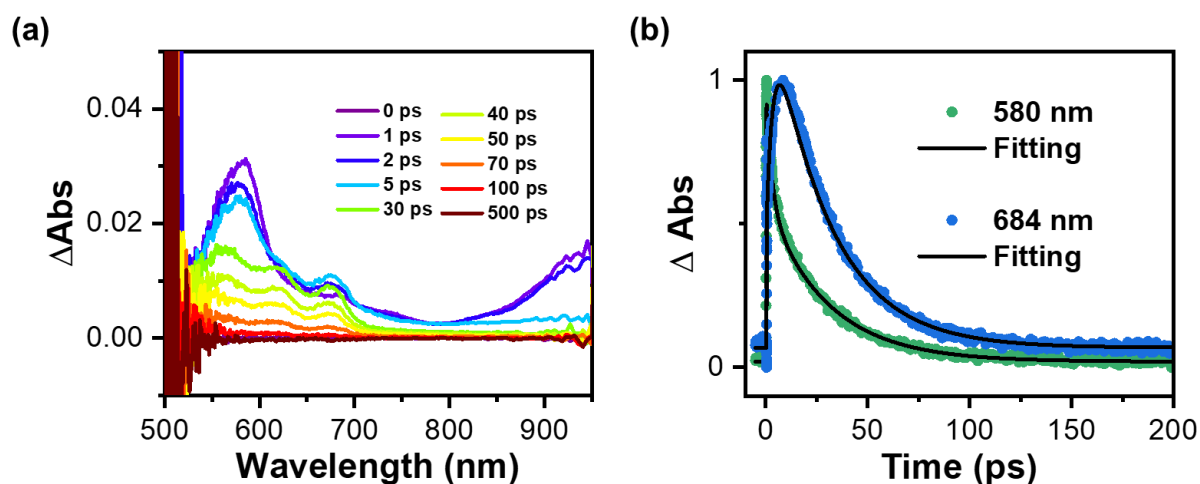
Fig. S34. Transient absorption data of **AbPP** in ACN. (a) transient absorption spectra at various delay times. (b) time traces at various probe wavelengths. The green data fitted to τ_{decay}=2.8 ps (decay of the LES and formation of the CSS and LEPT) along with a long decay component attributed to the CSS decay due to spectral overlap between the LES and CSS. The blue data fitted to τ_{rise}=4.7 (rise of the CSS) and τ_{decay}=26.4 ps (decay of the CSS).
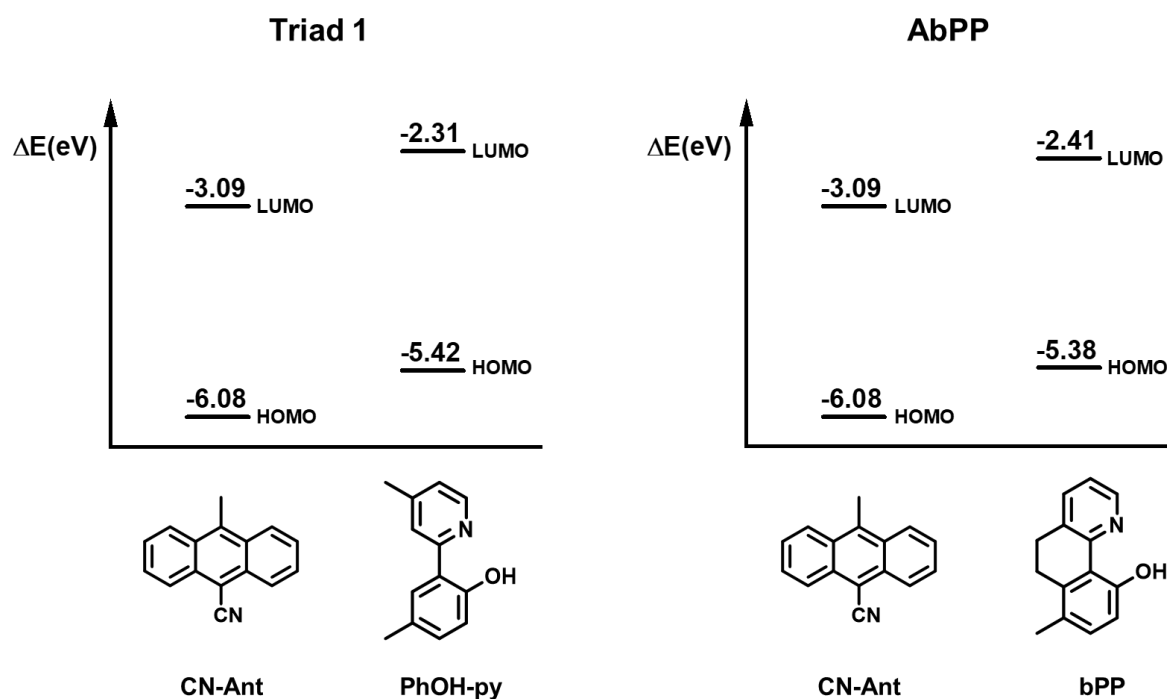

Fig. S35. The HOMO and LUMO energy level recorded by Cyclic voltammetry (CV) and differential pulse voltammetry (DPV) data of 10^{-3} M **bPP**, **PhOH-py**, and **CN-Ant.** CV and DPV were performed using Squidstat Plus with EIS (Admiral Instruments) and the software Squidstat User Interface v2.06.15.202. An Ag/AgCl was used as the reference electrode, Pt wire was used as the counter electrode and 0.1 M tetrabutylammonium hexafluorophosphate (TBAPF$_6$) was used as the supporting electrolyte. The oxidation potentials were investigated with a glassy carbon working electrode in

anhydrous DCM and reduction potentials were investigated with a glassy carbon working electrode in anhydrous DMF. All the scan rate was 100 mV/s.

5. Reference

1   Lian, X. *et al.* Siteselective and Enantiocomplementary C (sp3)–H Oxyfunctionalization for Synthesis of α-Hydroxy Acids. *ACS Catal.* **14**, 4463-4470 (2024).

2   Castillo-Rangel, N., Pérez-Díaz, J. O. H. & Vázquez, A. An expeditious synthesis of 8-Methoxy-1-tetralone. *Synth.* **48**, 2050-2056 (2016).

3   Okamoto, K., Watanabe, M., Murai, M., Hatano, R. & Ohe, K. Practical synthesis of aromatic nitriles via gallium-catalysed electrophilic cyanation of aromatic C–H bonds. *Chem. Commun.* **48**, 3127-3129 (2012).

4   Bowring, M. A. *et al.* Activationless multiple-site concerted proton–electron tunneling. *J. Am. Chem. Soc.* **140**, 7449-7452 (2018).

5   Parada, G. A. *et al.* Concerted proton-electron transfer reactions in the Marcus inverted region. *Science* **364**, 471-475 (2019).